

2021

## Effects of Fluoxetine/Simvastatin/Ascorbic Acid Combination Treatment on Neurogenesis and Functional Recovery in a Model of Multiple Sclerosis

Olivia Cameron Webb  
*Wright State University*

Follow this and additional works at: [https://corescholar.libraries.wright.edu/etd\\_all](https://corescholar.libraries.wright.edu/etd_all)



Part of the [Neuroscience and Neurobiology Commons](#), and the [Physiology Commons](#)

---

### Repository Citation

Webb, Olivia Cameron, "Effects of Fluoxetine/Simvastatin/Ascorbic Acid Combination Treatment on Neurogenesis and Functional Recovery in a Model of Multiple Sclerosis" (2021). *Browse all Theses and Dissertations*. 2432.

[https://corescholar.libraries.wright.edu/etd\\_all/2432](https://corescholar.libraries.wright.edu/etd_all/2432)

This Thesis is brought to you for free and open access by the Theses and Dissertations at CORE Scholar. It has been accepted for inclusion in Browse all Theses and Dissertations by an authorized administrator of CORE Scholar. For more information, please contact [library-corescholar@wright.edu](mailto:library-corescholar@wright.edu).

EFFECTS OF FLUOXETINE/SIMVASTATIN/ASCORBIC ACID COMBINATION  
TREATMENT ON NEUROGENESIS AND FUNCTIONAL RECOVERY IN A  
MODEL OF MULTIPLE SCLEROSIS

A thesis submitted in partial fulfillment of the  
requirements for the degree of  
Master of Science

by

CAMERON OLIVIA WEBB  
B.A., DePauw University, 2018

2021

Wright State University

WRIGHT STATE UNIVERSITY  
GRADUATE SCHOOL

July 15, 2021

I HEREBY RECOMMEND THAT THE THESIS PREPARED UNDER MY SUPERVISION BY Cameron Olivia Webb ENTITLED Effects of Fluoxetine/Simvastatin/Ascorbic Acid Combination Treatment on Neurogenesis and Functional Recovery in a Model of Multiple Sclerosis BE ACCEPTED IN PARTIAL FULFILLMENT OF THE REQUIREMENTS FOR THE DEGREE OF Master of Science.

---

Adrian Corbett, Ph.D.  
Thesis Director

---

Eric Bennett, Ph.D.  
Chair, Department of Neuroscience,  
Cell Biology, and Physiology

Committee on Final Examination:

---

Adrian Corbett, Ph.D.

---

Christopher Wyatt, Ph.D.

---

Sherif Elbasiouny, Ph.D.

---

Barry Milligan, Ph.D.  
Vice Provost for Academic Affairs  
Dean of the Graduate School

## ABSTRACT

Webb, Cameron Olivia. M.S., Department of Neuroscience, Cell Biology, and Physiology, Wright State University, 2021. Effects of Fluoxetine/Simvastatin/Ascorbic Acid Combination Treatment on Neurogenesis and Functional Recovery in a Model of Multiple Sclerosis.

Whereas immune modulation has proven beneficial in multiple sclerosis (MS), we hypothesized that targeting down-stream modulators of neurogenesis and subsequent remyelination may offer an additional, if not superior, point of intervention in an attempt to repair damage and recover lost function. As such, the present study assessed the effectiveness of 30-day administration of the drug combination fluoxetine (5 mg/kg), simvastatin (1 mg/kg), and ascorbic acid (50 mg/kg) (FSA) on an early marker of neurogenesis, doublecortin (DCX), and functional recovery using the Montoya Staircase following lysolecithin-induced focal demyelination of the corpus callosum in middle-aged (10-11 month) male and female rats.

Lysolecithin injection resulted in a functional deficit of about 27.5% for ipsilateral function and about 30% for contralateral function. Male control animals demonstrated a full recovery of function, for both ipsilateral and contralateral measures. Consistent with this finding, male controls also had the highest average DCX density/volume, although a significant correlation between the two measures was not seen. Male FSA animals also demonstrated recovery of function; however, it was blunted relative to male controls and did not reach pre-surgery baseline levels. Likewise, DCX density/volume was lower in

male FSA than male controls. Female control animals appeared to have impaired natural repair, demonstrating only limited functional recovery. After an initial larger functional deficit, female FSA animals showed functional recovery consistent with female controls for both ipsilateral and contralateral function, in neither case reaching pre-injury baseline performance. Consistent with the observed male to female functional differences, female DCX density and volume were significantly lower than in males. Taken together, these results indicate an innate difference in middle-aged male and female rat neurogenesis response to injury. The drug combination used in this study appeared to impair rather than augment recovery (both in terms of neurogenesis and function), a feature most pronounced in the male rats.

## TABLE OF CONTENTS

	Page
I. INTRODUCTION.....	1
Multiple Sclerosis.....	1
Types of MS.....	2
Effects of Aging on Disease Progression.....	6
Remyelination and Neurogenesis.....	6
Doublecortin.....	8
The Experiment.....	8
Lysolecithin.....	10
Hypothesis.....	11
II. METHODS.....	12
Animal Husbandry.....	12
Experimental Design.....	12
Lysolecithin-Induced Demyelination Surgery.....	14
Voluntary Oral Drug Administration.....	16
Montoya Staircase.....	17
Euthanasia and Cardioperfusion.....	20
Cryosectioning of Brain Tissue.....	21
DCX Antibody Staining.....	21
Tissue Mounting.....	24

TABLE OF CONTENTS (Continued)

	Image Analysis.....	24
	Statistical Analysis.....	25
	Montoya Staircase.....	25
	DCX Staining.....	25
	Correlation Studies.....	26
III.	RESULTS.....	27
	Montoya Staircase Functional Analysis.....	27
	DCX Staining Analysis.....	39
	Correlating DCX Staining and Functional Recovery.....	46
IV.	DISCUSSION.....	56
	Male Functional Recovery and Neurogenesis.....	57
	Female Functional Recovery and Neurogenesis.....	60
	Considerations for Future Studies.....	64
	Drug Combination and Dosage.....	64
	Timing of Group Assignment and Drug Initiation.....	65
	Timing of DCX Assessment.....	66
	Number of Animals and Animal Type.....	66
	Conclusion.....	67
V.	APPENDICES.....	68
	Appendix A: Male Montoya Staircase Raw Data.....	68
	Appendix B: Female Montoya Staircase Raw Data.....	70
	Appendix C: DCX Staining Raw Data.....	72

TABLE OF CONTENTS (Continued)

Appendix D: Oligo1 Staining Example.....	75
VI. REFERENCES.....	76

## LIST OF FIGURES

	Page
Figure 1.....	3
Figure 2.....	4
Figure 3.....	5
Figure 4.....	13
Figure 5.....	15
Figure 6.....	18
Figure 7.....	23
Figure 8.....	30
Figure 9.....	32
Figure 10.....	34
Figure 11.....	36
Figure 12.....	38
Figure 13.....	39
Figure 14.....	41
Figure 15.....	43
Figure 16.....	45
Figure 17.....	47
Figure 18.....	49
Figure 19.....	51

LIST OF FIGURES (Continued)

Figure 20.....	53
Figure 21.....	55

## LIST OF TABLES

	Page
Table 1.....	15
Table 2.....	27
Table 3.....	28
Table 4.....	40

## TABLE OF ABBREVIATIONS

ABC	Avidin/biotin complex
ANOVA	Analysis of Variance
AP	Anterior-Posterior
BDNF	Brain-derived neurotrophic factor
CIS	Clinically isolated syndrome
cm	Centimeter
CNS	Central nervous system
DAB	3,3'-Diaminobenzidine
DCX	Doublecortin
DPX	Dibutylphthalate Polystyrene Xylene
eNOS	Endothelial nitric oxide synthase
FDA	Food and Drug Administration
FSA	Fluoxetine/Simvastatin/Ascorbic acid
HMG-CoA	3-hydroxy-3-methylglutaryl-CoA
IACUC	Institutional Animal Care and Use Committee
IgG	Immunoglobulin G
IP	Intraperitoneal
kg	Kilogram
LAR	Laboratory Animal Resources
MAP	Microtubule-associated protein
mg	Milligram
ml	Milliliter
ML	Medial-Lateral

mm	Millimeter
MRI	Magnetic resonance imaging
MS	Multiple sclerosis
NIH	National Institutes of Health
NO	Nitric oxide
OCT	Optimal cutting temperature
OPC	Oligodendrocyte progenitor cell
PBS	Phosphate buffered saline
PPMS	Primary progressive multiple sclerosis
PSD	Post-surgery day
ROS	Reactive oxygen species
RRMS	Relapsing-remitting multiple sclerosis
SE	Standard error
SEM	Standard error of the mean
SGZ	Subgranular zone
SPMS	Secondary progressive multiple sclerosis
SSRI	Selective serotonin reuptake inhibitor
SVZ	Subventricular zone
TNF- $\alpha$	Tumor necrosis factor - $\alpha$
tPA	Tissue-type plasminogen activator
$\mu$ l	Microliters
$\mu$ m	Micrometers (or microns)

## ACKNOWLEDGEMENTS

I would first like to thank my advisor, Dr. Adrian Corbett, for her continued support and guidance throughout my master's education, as well as development of this project. Her patience in teaching me the necessary skills required to conduct scientific research, as well as her flexibility and willingness to help in any way throughout the coronavirus pandemic has been greatly appreciated. I would also like to acknowledge my fellow students working in Dr. Corbett's lab, especially Teshawn Johnson on her work with the Oligo1 staining. Even though we did not get to spend time together in the lab due to the global pandemic, the contributions and flexibility from each student allowed us to complete this project.

Additionally, I would like to thank my father for his guidance, support, and encouragement. His knowledge and experience have helped me gain a better understanding of the scientific world. I am extremely grateful for the unconditional love and support both my parents have given me.

Lastly, I would like to acknowledge my wonderful husband, Ray. He has supported me through all the ups and downs of my graduate education, providing me with continuous love, encouragement, and kindness. His unwavering confidence in my knowledge and abilities has always amazed me, and I will always be grateful for him.

## I. INTRODUCTION

### *Multiple Sclerosis*

Multiple Sclerosis (MS) is an inflammatory neurological disease characterized by an immune system attack of myelinated axons in the central nervous system (CNS), resulting in damage to white matter tracts, or demyelination. While MS generally has an onset in young adulthood, the average age of individuals with MS is rising (1). The exact cause of the disease is not fully understood, but it is thought that a combination of genetic predisposition and environmental factors contribute to disease onset (2, 3).

Environmental factors that appear to be the most convincing risk factors are low vitamin D levels, cigarette smoke, Epstein-Barr virus infection, and obesity (2, 4).

The prevalence of MS is higher in females than males, with an estimated ratio of 3:1 (4-6). While the reason for this is not fully understood, there is evidence that sex hormones could play a role (5). Pregnancy has been seen to reduce relapses (5-7), possibly due to the high levels of hormones, especially estrogens (5). While there have not been extensive studies on the effects of loss of sex hormones during menopause, it is thought that it does not have an effect on disease susceptibility because disease onset generally takes place before menopause (7). However, sex hormone changes and fluctuations may affect disease progression. Women report more severe symptoms prior to menstruation when estradiol levels are low and worsening disabilities with menopause (7, 8). This increase in MS symptoms following menopause suggests that the loss of

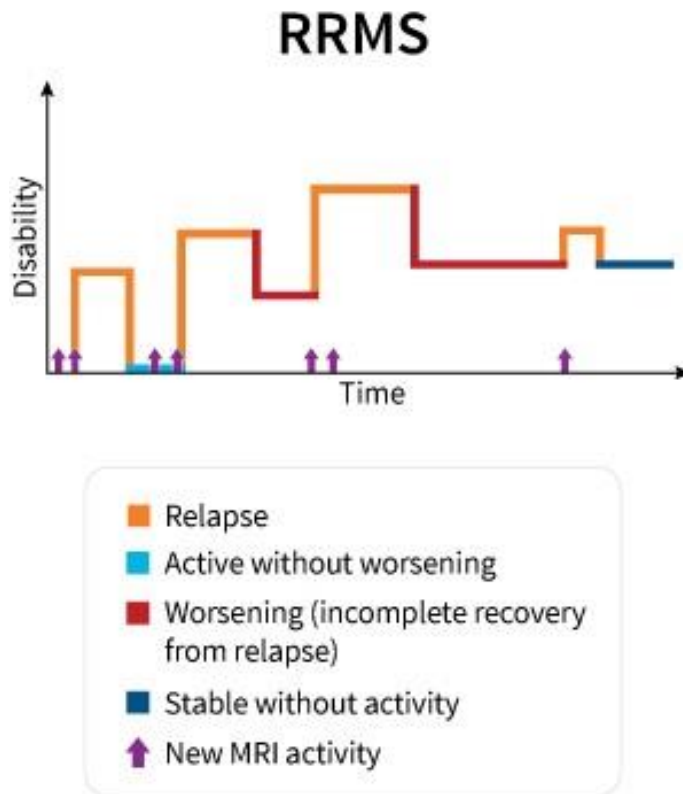
hormones could be causally linked to neurodegeneration in secondary progressive MS (6).

### ***Types of MS***

There are currently four subtypes, or disease courses, of MS that have been defined by the International Advisory Committee on Clinical Trials of MS in 2013: Clinically isolated syndrome (CIS), relapsing-remitting MS (RRMS), primary progressive MS (PPMS), and secondary progressive MS (SPMS) (9).

CIS is an initial episode of disease symptoms caused by inflammation or demyelination and lasting at least 24 hours (10). Individuals with CIS do not yet meet the requirements for MS and may or may not develop the disease over time. If CIS becomes active and fulfills current diagnostic criteria for MS, it becomes RRMS (11).

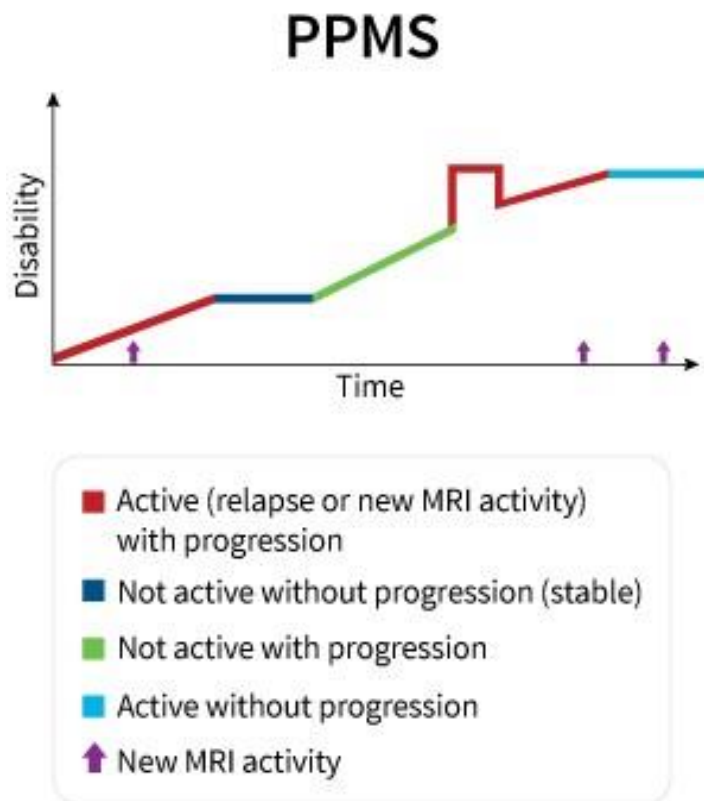
RRMS is the most common type of MS, with approximately 85% of MS patients initially being diagnosed with this disease course (3, 10). As depicted in Figure 1, it is characterized by attacks, or relapses, of neurological dysfunction, followed by periods of remission, where symptoms are improved or completely disappear (10). The disease does not appear to progress during the periods of remission. RRMS is further characterized as active or not active, and worsening or not worsening. Active indicates relapses or new/larger lesions seen as new MRI activity, and worsening indicates an increase in impairment/disability following relapse (9, 10).



Source: Lublin et al., 2014.

**Figure 1:** Example characterizing key features of RRMS. Image source: National Multiple Sclerosis Society (12).

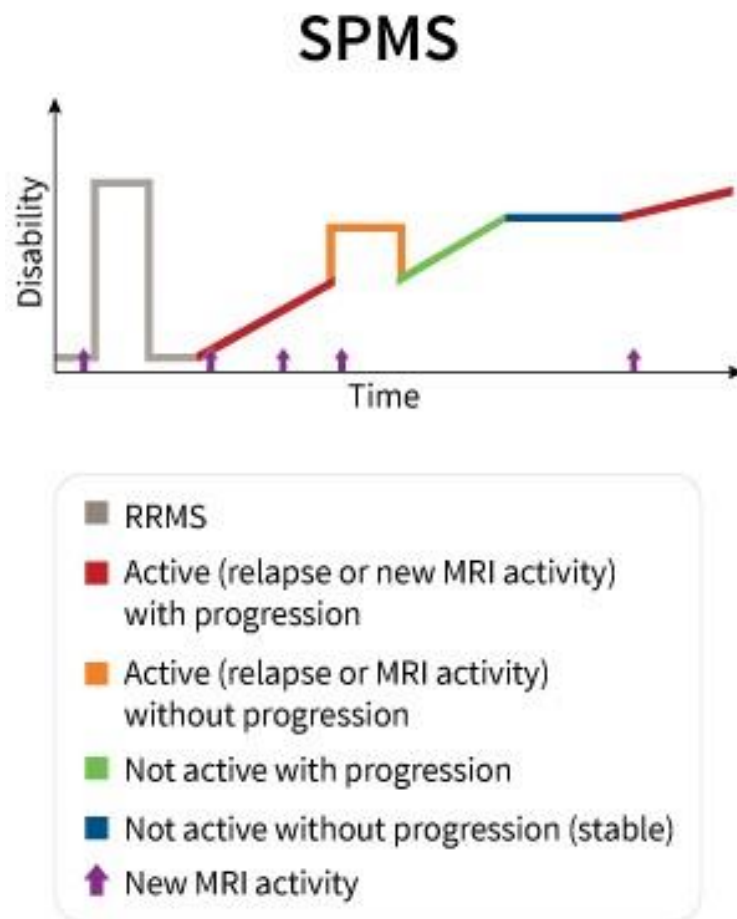
PPMS affects approximately 10% - 20% of people with MS, and is characterized by gradual worsening of symptoms, or accumulation of disability, from disease onset, without relapses or remissions (10), as depicted in Figure 2. PPMS is further characterized as active or not active, and with progression or without progression. Active indicates occasional relapses or new/larger lesions seen as new MRI activity, and with progression indicates accumulation of disability over time, with or without relapses (9, 10).



Source: Lublin et al., 2014.

**Figure 2:** Example characterizing key features of PPMS. Image source: National Multiple Sclerosis Society (13).

SPMS begins as RRMS, then neurological function progressively declines, and disability accumulates over time (10), as depicted in Figure 3. The main difference between SPMS and PPMS is the lack of relapses prior to progression in PPMS (11). Similar to PPMS, SPMS can be further characterized as active or not active, and with progression or without progression.



Source: Lublin et al., 2014.

**Figure 3:** Example characterizing key features of SPMS. Image source: National Multiple Sclerosis Society (14).

### ***Effects of Aging on Disease Progression***

Most MS patients, especially those diagnosed as young adults, initially suffer from RRMS, with relapses and remissions, followed by progression into SPMS (15). It should be noted, however, that not all patients with RRMS will develop SPMS (1). Age has been shown to be the greatest predictor for the transition from RRMS to SPMS (15). It has also been shown that PPMS typically occurs at an older age than RRMS (1, 15, 16). This indicates that age is a very important risk factor for developing more progressive forms of MS.

In MS, the brain naturally attempts to remyelinate axons following demyelinating inflammation. As a person ages, this ability to remyelinate gradually decreases, which is thought to contribute to the failed remyelination in progressive MS (15, 16). Several animal models of demyelination have shown that aging reduces the capacity for remyelination due to impaired recruitment and maturation of oligodendrocyte progenitor cells (OPCs) in the demyelinated areas (1, 15). Additionally, aging is associated with a decrease in neurogenesis (15), which could also be a contributing factor in the deteriorating ability to remyelinate.

### ***Remyelination and Neurogenesis***

In MS, inflammation results from the activation of the immune system. This immune response activates microglia in the CNS tissue from the resting state into the M1 pro-inflammatory subtype (17). Microglia in the M1 state are associated with increased pro-inflammatory cytokine production, including tumor necrosis factor- $\alpha$  (TNF- $\alpha$ ), nitric oxide (NO), and reactive oxygen species (ROS) (18). Under normal conditions, M1

microglia help protect neurons and provide defense against diseases and invading pathogens, but excessive inflammation can lead to neuronal damage and loss and neurodegenerative diseases (18). In order to induce remyelination in MS, the microglia need to be shifted from the M1 subtype to the M2 anti-inflammatory subtype. M2 microglia secrete anti-inflammatory cytokines and growth factors, including brain-derived neurotrophic factor (BDNF), and they promote tissue repair and remyelination (17). BDNF is a growth factor that has been associated with cell survival, increased neurogenesis, enhanced learning and memory, and promotion of neuroplasticity (19).

Neurogenesis occurs in two niches in the adult mammalian brain: the subventricular zone (SVZ) of the lateral ventricles and the subgranular zone (SGZ) of the dentate gyrus in the hippocampus (20, 21). Generally, neuroblasts originating in the SVZ travel to the olfactory bulb. However, studies have shown that the subventricular zone can respond to brain injury, causing neuroblasts to migrate to the injured area (22, 23). Cells originating in the SVZ migrate to the injured area and then are able to differentiate into neurons and glia (particularly oligodendrocytes) (23, 24). There is evidence that neurogenesis in the subventricular zone can lead to increased oligodendrocyte proliferation, and these oligodendrocytes can contribute to remyelination (23, 25-27). However, as cited above, aging is associated with decreased neurogenesis (15). In middle-aged patients with MS, the decrease in neurogenesis could result in decreased ability to remyelinate damaged areas of the brain. In order to increase remyelination to treat MS, it may be suggested that it is first necessary to increase neurogenesis in the brain. Increased neurogenesis and remyelination is expected to lead to functional recovery of the injured area of the brain. As such, the principle aim of this study was to

examine if a specific drug combination would enhance neurogenesis and promote recovery of lost function in an experimentally induced rodent model of MS.

### ***Doublecortin***

Doublecortin (DCX) is a microtubule-associated protein (MAP) that is expressed in newly born neuroblasts and migrating neuroblasts, making it an important marker for adult neurogenesis (28-30). Progenitor cells migrating from the SVZ will express DCX prior to differentiating into neurons or glia. DCX is expressed in these new migrating cells for 2-3 weeks but decreases as the neuroblast matures and starts expressing markers of mature neurons or oligodendrocytes (29, 31). Furthermore, the expression of DCX is downregulated in OPCs (29). Due to the transient expression of DCX, it is a well-known marker for adult neurogenesis.

### ***The Experiment***

To date, all therapies that have been approved by the U.S. Food and Drug Administration (FDA) to treat MS modulate the immune system. Whereas immune modulators represent a logical point of intervention, we hypothesized that targeting remyelination of damaged white matter tracts will also be important for arresting disease progression, and additionally holds potential for repairing lost function.

The drugs included in this study were fluoxetine, simvastatin, and ascorbic acid. This drug combination was selected because it has been shown to increase functional recovery of damaged white matter tracts in the corpus callosum of female rats in an ischemic stroke model (32). The anticipated effects in male rats were less clear, as the

drugs simvastatin and fluoxetine independently appear to reduce neurogenesis in a non-injury model (33), whereas fluoxetine, simvastatin, and ascorbic acid in combination appear to enhance neurogenesis in an ischemic stroke model (32). Recovery was assessed through the measurement of the biomarker DCX, and functional evaluation using the Montoya Staircase behavioral test.

The first drug in our combination was fluoxetine. Fluoxetine is a selective serotonin reuptake inhibitor (SSRI) that is generally prescribed to treat depression, but it has been found to also reduce brain damage in ischemic stroke and exert anti-inflammatory effects (34). Studies suggest fluoxetine can change M1 microglia into M2 microglia and also possibly reduce blood brain barrier permeability. This latter drug-effect potentially aids the remyelination process by inhibiting peripheral immune cell migration into the brain, thus reducing an additional source of inflammation and damage (35, 36). Transitioning microglia into the M2 state will help promote healing and repair, as previously mentioned, through the release of anti-inflammatory cytokines and growth factors.

The second drug in our combination was simvastatin. Simvastatin, an HMG-CoA reductase inhibitor, has been shown to increase the expression of BDNF following brain injury (24, 37) and promote proliferation and differentiation of oligodendrocyte precursors (24, 38). It has also been shown to increase endothelial nitric oxide synthase (eNOS) and upregulate tissue-type plasminogen activator (tPA), which cleaves plasminogen to form plasmin (39, 40). Plasmin cleaves pro-BDNF, which is the BDNF precursor, to the mature form of BDNF (41, 42). Pro-BDNF has been shown to have opposing effects to mature BDNF, promoting apoptosis and deterioration of synaptic

function (42, 43). Thus, cleaving pro-BDNF to mature BDNF is important to promote neurogenesis and cell survival. Simvastatin is currently being tested in a clinical trial for progressive MS (44). Alternatively, some studies suggest that long-term use (5 weeks) of simvastatin (2 mg/kg) inhibits remyelination by preventing OPCs from maturing into myelinating oligodendrocytes (44, 45). Findings from these studies, however, are potentially confounded by IP administration of the drug, which could result in stress related inhibition of neurogenesis (46-50). In the present investigation simvastatin was included at a lower dosage (1 mg/kg) and in combination with fluoxetine and ascorbic acid.

Ascorbic acid, or vitamin C, was included as the final drug in our combination because it has been shown to promote differentiation of oligodendrocyte precursors to mature oligodendrocytes and promote remyelination (33, 51). The exact mechanisms by which it promotes differentiation and maturation of oligodendrocytes is not known, but it is thought to be unrelated to its antioxidant properties (51).

### ***Lysolecithin***

Lysolecithin is a toxin commonly used to study demyelination and remyelination processes. Lysolecithin causes focal demyelination by killing oligodendrocytes and selectively destroying myelin at the site of injection and the immediately surrounding area (52). The exact mechanism by which it causes demyelination is not fully understood, but it is thought that its lipid-disrupting properties likely induces toxicity (53). Due to the focal lesion caused by this agent, it is commonly used to test therapies for remyelination.

### *Hypothesis*

We hypothesized that the use of the drug combination fluoxetine, simvastatin, and ascorbic acid would increase neurogenesis in the subventricular zone, stimulating remyelination of injured axons, and ultimately result in improved functional recovery in a lysolecithin-induced demyelination model of multiple sclerosis.

## II. METHODS

### *Animal Husbandry*

Male (N = 20) and female (N = 20) Sprague Dawley rats, 10-11 months old (middle age), were used in this study. Rats were individually housed in standard cages with wood chip bedding. They were provided ad libitum access to food and water, 24 hours per day, 7 days per week, except during periods of Montoya Staircase training and testing (as described). The animal room was maintained on a 12-hour light/ 12-hour dark cycle at approximately 74°F. Animals were fasted 7-8 hours preceding Montoya Staircase training and testing, then food was restricted to 85% ad lib during the training and testing days, so that animals were not satiated during testing, thereby circumventing the treat reward. All animal husbandry practices and experimental procedures (described below) were approved by the Wright State University Institutional Animal Care and Use Committee (IACUC).

### *Experimental Design*

Animals arrived at the Laboratory Animal Resources housing facility (LAR) at Wright State University and were given five days to acclimate to their new environment. They were then trained to perform the Montoya Staircase test, and functional baseline performances were determined. Animals incapable of learning the Montoya Staircase were removed from the study (N = 2 males, N = 2 females). All remaining animals then underwent a lysolecithin-induced demyelination surgery (described below), and were

subsequently divided into four groups: male control (N = 8), male fluoxetine/simvastatin/ascorbic acid (FSA) (N = 10), female control (N = 8), and female FSA (N = 10). These animals received either vehicle control or the drug regimen (combined 5 mg/kg fluoxetine, 1 mg/kg simvastatin, 50 mg/kg ascorbic acid) for 32 days, beginning approximately 24 hours after the demyelination surgery. To determine functional recovery following surgery, animals were tested using the Montoya Staircase on post-surgery days 3-5, 15-17, and 30-32. Animals were euthanized on post-surgery day (PSD) 33 using Euthasol injection, followed by cardioperfusion, then decapitation and dissection of the brain. The tissue was then sliced and stained with DCX primary antibody, as a marker of neurogenesis. Staining was followed by tissue mounting onto slides. A timeline of the present study is provided in Figure 4.

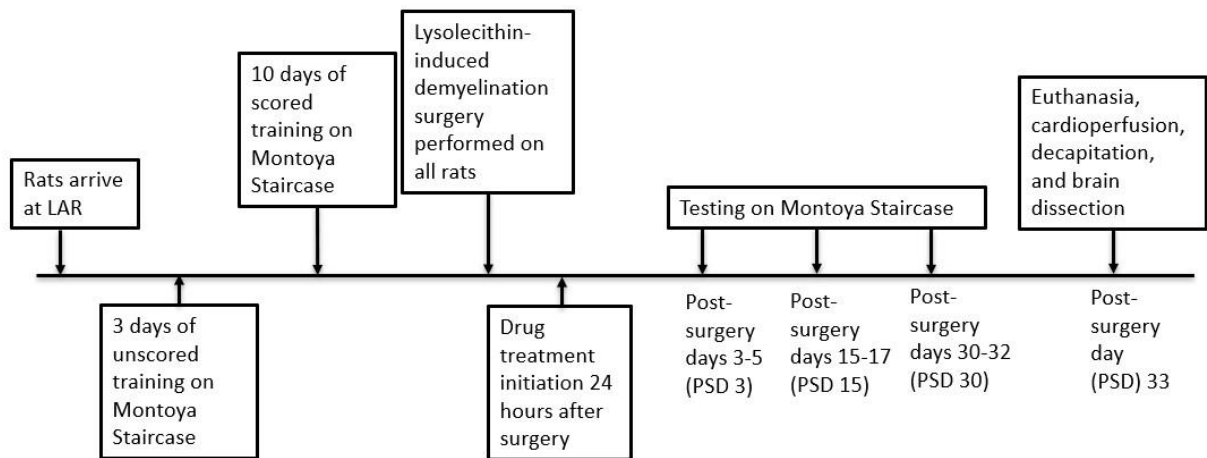


**Figure 4:** Timeline of the present experiment.

### ***Lysolecithin-Induced Demyelination Surgery***

All animals, except the previously mentioned four animals deemed incapable of learning the Montoya Staircase, received the lysolecithin-induced demyelination surgery. Rats were initially anesthetized in an induction chamber using 5% isoflurane gas. Animals were then prepared for surgery (head shaved) and mounted into a stereotactic apparatus, using non-traumatic ear bars and a tooth hold to stabilize the head. Rats were maintained under anesthesia throughout the procedure using 2.5% isoflurane gas delivered through a nose cone. A glove was tied under the rat's chin (around the nose cone) to make sure it was not able to breathe the air from the room. Eye lube was applied to each eye to prevent them from drying out during the surgery. Provoiodine was scrubbed on the surgical area to clean it, followed by 70% ethanol, then a final coat of provoiodine was added. An incision was made down the midline of the skull, extending to the end of the eyes, and a few drops of bupivacaine (0.25%), an analgesic, was added to the incision site. Blood was cleared with a cotton swab until the skull was exposed. Bregma, an area of the skull where the bone plates fuse, was located and marked with a fine tip permanent marker. A micro drill was mounted on the stereotactic apparatus, enabling precise alignment of the drill bit relative to Bregma. Once over Bregma, the anterior-posterior (AP) and medial-lateral (ML) coordinates were dialed-in and recorded (as noted in Table 1), and two holes were drilled. Figure 5 illustrates the location of Bregma, along with the locations of the two drill holes (shown in red).

**Table 1:** Drill hole coordinates for lysolecithin injection.

	AP Position from Bregma	ML Position from Bregma
Male First Hole	0 cm	0.27 cm
Male Second Hole	0.15 cm	0.27 cm
Female First Hole	0 cm	0.25 cm
Female Second Hole	0.15 cm	0.25 cm

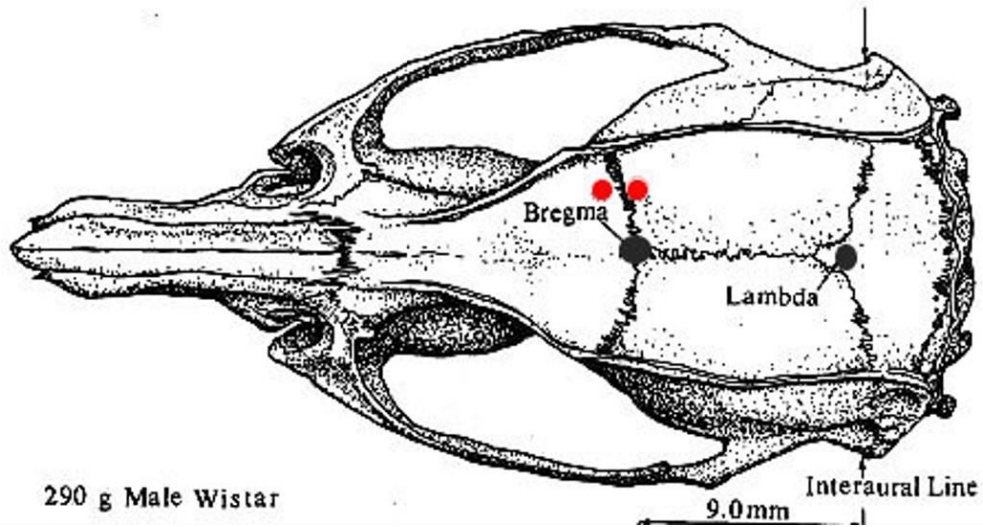


**Figure 5:** Location of two drill holes (red) relative to Bregma in male rat.

After holes had been drilled at the two locations, the drill was removed from the stereotactic apparatus and replaced with a Hamilton syringe. The syringe, which was filled with 3  $\mu$ l of 1% lysolecithin, was positioned just inside the first hole and the depth at the top of the brain was recorded. We subtracted 0.29 cm for males and 0.27 cm for females from the recorded depth and lowered the syringe until reaching that calculated depth. Once the syringe reached the appropriate depth, lysolecithin was slowly injected, about 0.1  $\mu$ l added every 20 seconds, until 1.5  $\mu$ l was added. The same procedure was then used to inject lysolecithin into the second hole. After lysolecithin injection into both holes, the incision was closed with 4-5 sutures, and povidone iodine applied to the region to prevent contamination. The isoflurane was then turned off, and oxygen was supplied. The glove tied around the nose cone and ear bars were removed. Once the animal started moving, it was removed from the nose cone and placed back in its cage, which was positioned on a heating pad. The animal remained in its cage on the heating pad until normal movement around the cage was observed, at which point the animal was returned to its normal housing area. Acetaminophen (200 mg/kg) was given in sugar cookie dough the day of surgery and the day after surgery.

### ***Voluntary Oral Drug Administration***

The drug combination, provided each morning starting approximately 24 hours after surgery and continued daily until the end of the study period, was administered to the rats inside a 4 gram sugar cookie dough ball (vehicle control) to prevent stress, as described previously (50). 5 mg/kg fluoxetine (Prozac), 1 mg/kg simvastatin, and 50 mg/kg ascorbic acid were weighed and inserted into the cookie dough. Animals in the

control group were given the 4 gram sugar cookie dough ball with nothing inside. All animals voluntarily consumed the cookie dough. Animals were not given drugs on the day of euthanasia.

### ***Montoya Staircase***

Montoya Staircase was used to evaluate fine motor control by measuring grasping ability in each forepaw. The apparatus, as seen in Figure 6, contains a platform, which holds the rat's body, with seven graded steps going down each side, allowing assessment of grasping ability in each forepaw independently. The well on each step was filled with three 50 mg banana flavored sucrose pellets, totaling 21 pellets on each side. For the first three days of training, unscored training took place during the light cycle to encourage animals to come out onto the platform and eat the sucrose pellets. Scored training took place during the dark cycle (in the evening). During training, food was restricted to 85% ad lib feed, and animals were fed each day at the end of the training session. Following the last training session, food was returned to ad lib. The training consisted of one 15-minute test per day, per rat, for 10 days. The training tests were scored as the number of pellets per paw that the animal retrieved. The data from the last three days of training were averaged to determine the baseline normal function for each rat. Animals that were unable to learn the Montoya Staircase (did not demonstrate the ability to pick up at least 9 pellets per paw) were excluded from analysis.

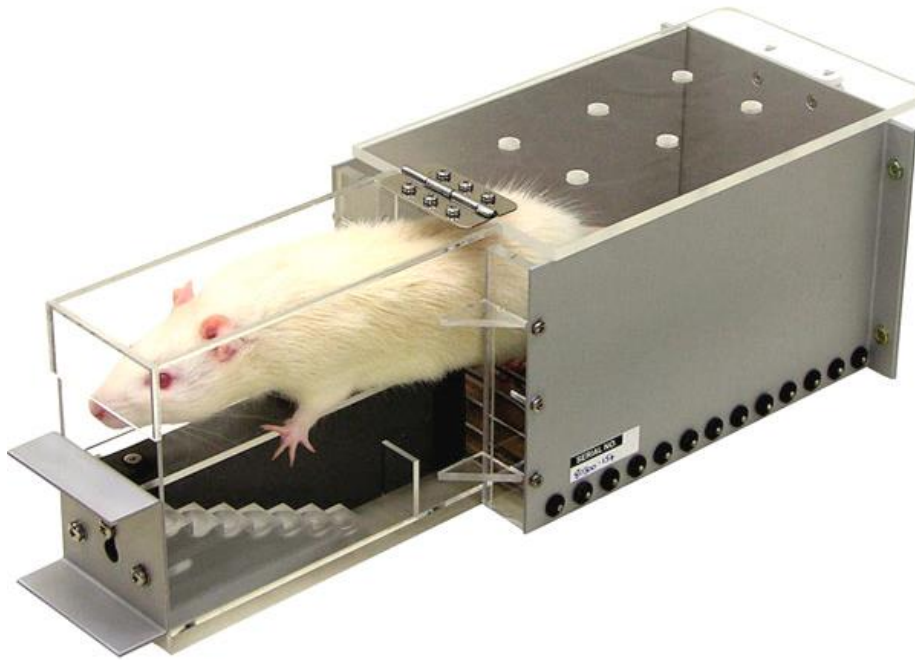


**Figure 6:** Image showing rat in the Montoya Staircase apparatus. Adapted from Lafayette Instrument Company (54).

The animals were tested on the Montoya Staircase on post-surgery days 3-5, 15-17, and 30-32. Each period of three-day testing consisted of one 15-minute test per day, per rat, for three days. All tests were performed during the dark cycle. During testing, food was restricted to 85% ad lib feed with animals being fed in the evening after each testing session. Following the test on the third day, animals were returned to ad lib food. The data for those three days were averaged to get one value per period (post-surgery day 3, post-surgery day 15, and post-surgery day 30). This average value for each animal was divided by its normal baseline number of pellets grabbed (pre-surgery baseline normal function) to determine functional deficit and functional recovery (as shown in the

equations below). Calculations were performed for ipsilateral function (right side forepaw) and contralateral function (left side forepaw).

The ipsilateral and contralateral function and deficit were calculated as follows:

$$\text{Ipsilateral function (PSD \#)} = \frac{\text{Average number of pellets (PSD \#) (Right)}}{\text{Baseline normal function (Right)}}$$

$$\text{Contralateral function (PSD \#)} = \frac{\text{Average number of pellets (PSD \#) (Left)}}{\text{Baseline normal function (Left)}}$$

$$\text{Ipsilateral Deficit} = 1 - \text{Ipsilateral function (PSD 3)}$$

$$\text{Contralateral Deficit} = 1 - \text{Contralateral function (PSD 3)}$$

Ipsilateral and Contralateral recovery were calculated as follows:

$$\text{Ipsilateral Recovery (PSD 30)} =$$

$$\text{Ipsilateral function (PSD 30)} - \text{Ipsilateral function (PSD 3)}$$

$$\text{Contralateral Recovery (PSD 30)} =$$

$$\text{Contralateral function (PSD 30)} - \text{Contralateral function (PSD 3)}$$

Functional analysis resulting in a value less than one registers as a functional deficit for that paw. For example, a functional value of 0.80 for the ipsilateral paw on PSD 3, equates to this animal having 80% of its normal function, thus displaying a 20% functional deficit. Repeated measures, on PSD 15 and PSD 30, allowed for evaluation of recovery of function.

### ***Euthanasia and Cardioperfusion***

The animals were all euthanized 33 days post-surgery. Each animal was individually taken into the necropsy room for euthanasia. The animals were administered an IP injection of pentobarbital (100-150 mg/kg Euthasol). Once the animal showed no sign of response to a strong tail pinch, an incision was made to open the chest cavity and a catheter was placed in the apex of the left ventricle of the heart. Phosphate buffered saline (PBS) was then flushed through the catheter (about 150 ml), and a cut in the right atria was made to allow the blood to be drained from the body. Once the blood was cleared from the body, 4% paraformaldehyde in PBS was infused to fix the tissue, running approximately 150 ml through the tissues until the body was stiff. The rat's head was decapitated, and the brain dissected. The brain was left in 4% paraformaldehyde PBS in the refrigerator. After 24 hours had passed, the brain was switched into 30% sucrose solution for three days prior to cryosectioning. When first placed in the sucrose, the brain was floating. Once the sucrose permeated the brain tissue, the brain sank to the bottom of the container, indicating it was ready to be cut.

### ***Cryosectioning of Brain Tissue***

The dissected brains were removed from sucrose and prepared for cryosectioning by first gluing the brain onto a Peltier device with optimal cutting temperature (OCT) compound. The Peltier, with the brain and OCT compound combination, was placed in the cryostat on the Peltier cooling device to completely freeze the brain and OCT compound. Roughly 20 minutes were needed to freeze the tissue and compound to the same temperature as the temperature of the cryostat (-25°C) in order to slice the sections without causing damage. The brain was then loaded into the pedestal support and cut into coronal slices 50 µm in thickness. The sliced sections were sequentially placed and stored in vials containing PBS for subsequent biomarker analysis.

### ***DCX Antibody Staining***

For DCX staining, the PBS in the vials was removed and Bloxall was added until all sections were covered. The vials were incubated for 10 minutes, then washed with PBS. Blocking solution was then added (PBS with 0.3% Tween and 3% goat serum) to all sections (1 ml for test samples) and let incubate for one hour. Then a 1:1500 dilution (0.67 µl per 1 ml) of DCX primary antibody (Rabbit anti-DCX IgG, Cell Signaling Technology #4604S) was added directly to blocking solution in the specimen vials and incubated for 30 minutes. After 30 minutes of incubation, the primary antibody solutions were removed. Sections were washed with 3-5 ml PBS-Tween twice. Then 1 ml blocking solution was added to the specimen vials, followed by 5 µl of a secondary biotinylated goat anti-rabbit antibody (Vector ABC kit). The vials were then incubated for 30 minutes at room temperature, then washed twice with 3 ml PBS-Tween. Vials were then

incubated with Avidin/Biotin complex (ABC) solution (1 ml) (system shown in Figure 7) for 30 minutes, then washed two times with 3 ml PBS-Tween. The 3,3'-Diaminobenzidine (DAB) solution with nickel was then added (1 ml per vial), and after 10 minutes of incubation the solution was removed and replaced with distilled water. Background control specimen vials were prepared identically to the DCX specimen vials, albeit with no primary antibody incubation step.

Using the ABC System:

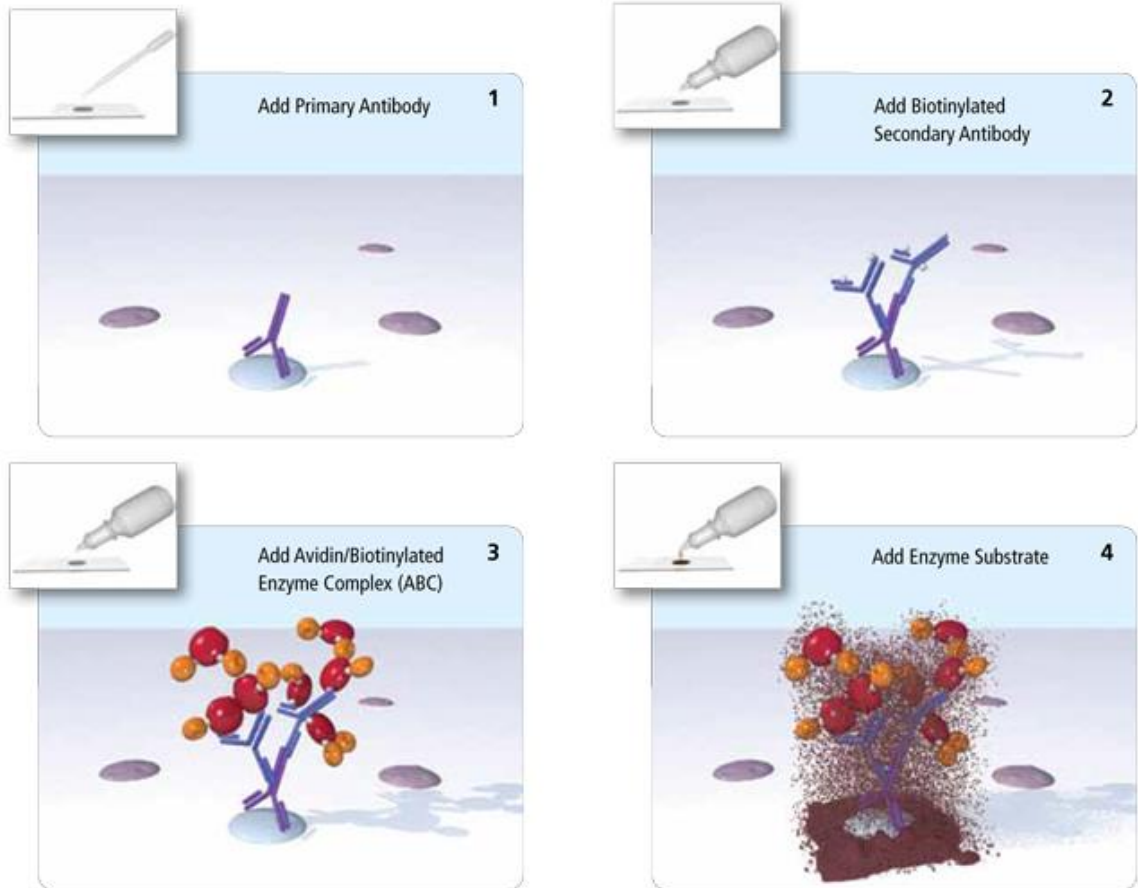


**Figure 7:** Avidin Biotin Complex (ABC) solution process. For this study, the secondary antibody was biotinylated goat antibody to rabbit IgG, and the enzyme substrate was the DAB solution. Image retrieved from <https://vectorlabs.com/vectastain-elite-abc-kit-standard.html> (55).

### ***Tissue Mounting***

The vials containing the DCX stained tissue slices and control tissue slices were emptied into individual petri dishes that contained PBS. The slices were mounted onto gel-coated slides using a thin tip paintbrush. About 4-6 slices were mounted on each slide, being careful to prevent folding or tearing. Once the tissues were dry, DPX mountant (Sigma-Aldrich) was applied over the sections to preserve staining, and a coverslip was placed on top to cover all the sections on the slide.

### ***Image Analysis***

Each slide was examined, in a blinded manner, using the 4X objective lens on a bright-field microscope and ToupView visualization software to assess DCX staining along the subventricular zone. The DCX stain appeared as a dark purple color. Most brain slices were too large to be captured by a single photo, therefore multiple images were taken of each section. Individual magnified digital images were taken of each ventricle and surrounding area and merged/blended in Adobe Photoshop to create one large image showing both ventricles of each brain slice. The images were saved and labeled by the rat's identification number, the slide number, and the numbered position on that slide. The images were converted into grayscale using Adobe Photoshop. The grayscale images were used to make a mask in the NIH Image J program that highlighted the DCX staining. The freehand tool was used to enclose the specific area of the ventricle that contained staining, allowing quantification of the DCX staining area. Control tissues were all clean (did not have any stain), and therefore were not used in the quantification of DCX. DCX staining was quantified as pixels/mm<sup>2</sup> for each brain slice assessed.

Overall density, the average pixels/mm<sup>2</sup> for each brain slice for both ventricles, was expressed as mm<sup>2</sup>/ventricle. Total volume was calculated as total area (sum of pixel/mm<sup>2</sup> for each brain slice for both ventricles) multiplied by the thickness of each slice (50 microns) multiplied by the number of vials that brain sections were distributed in for immunocytochemistry staining (8) and expressed as mm<sup>3</sup>.

### ***Statistical Analysis***

#### ***Montoya Staircase***

Functional results for the Montoya Staircase were compiled in a Microsoft Excel data table. Mean  $\pm$  SE was calculated for each group (male control, male FSA, female control, female FSA), for each test period (PSD 3, PSD 15, PSD 30), for both ipsilateral and contralateral responses. Two-way repeated measures analysis of variance (ANOVA) was used to assess treatment effects for ipsilateral and contralateral conditions in males and females independently (SigmaStat). To isolate which groups differ from the others the Holm-Sidak Multiple Comparison method was used, with significance set at  $P < 0.05$ .

#### ***DCX Staining***

DCX staining measurements (total volume and average density) were compiled in a Microsoft Excel data table. Mean  $\pm$  SE was calculated for each group (male control, male FSA, female control, female FSA). A two-way analysis of variance (ANOVA) was used to assess treatment effects (SigmaStat). To isolate which groups differ from the others the Holm-Sidak Multiple Comparison method was used, with significance set at  $P < 0.05$ .

### Correlation Studies

Ipsilateral functional recovery and contralateral functional recovery at PSD 30 were calculated and compiled in a Microsoft Excel data table. Correlation analysis was performed to determine the relationship between DCX volume and ipsilateral functional recovery at PSD 30 and DCX volume and contralateral functional recovery at PSD 30 for male control, male FSA, female control, and female FSA groups. An online Pearson correlation coefficient calculator was used to determine the R value, the  $R^2$  value, and the P value for each correlation analysis.

### III. RESULTS

#### *Montoya Staircase Functional Analysis*

Functional performance of fine motor control, grasping, at baseline, days 3-5 post-demyelination surgery, and at days 15-17 and 30-32 of recovery was assessed using the Montoya Staircase. Performance outcomes, measured as the number of sucrose pellets retrieved per forepaw, were averaged across the 3-day testing periods for each rat and expressed as PSD 3, PSD 15, and PSD 30. Functional deficit (at PSD 3) and functional recovery (at PSD 30) were then calculated, as described in Methods. Performances for ipsilateral function (right side paw) and contralateral function (left side paw) were measured. Initial deficits are noted in Table 2 below.

**Table 2:** *Initial deficits for male control, male FSA, female control, and female FSA groups.*

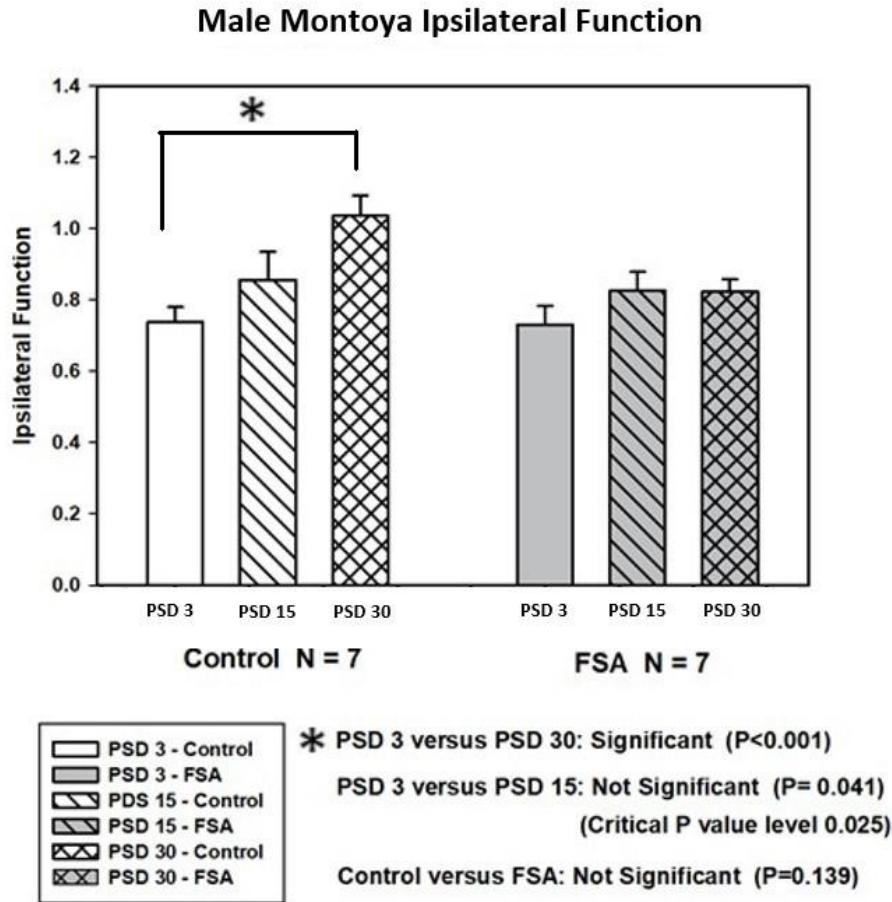
	Ipsilateral Deficit	Contralateral Deficit
Male Control	26%	16%
Male FSA	27%	35%
Female Control	21%	29%
Female FSA	36%	50%

Animals that did not show an initial functional deficit in either ipsilateral side alone or both ipsilateral and contralateral sides following post-surgery day 3 testing were excluded from analysis. This included four male rats and seven female rats. Table 3 shows the test groups remaining for final Montoya Staircase analysis once exclusions were applied.

*Table 3: Test groups for final Montoya Staircase analysis following application of exclusions.*

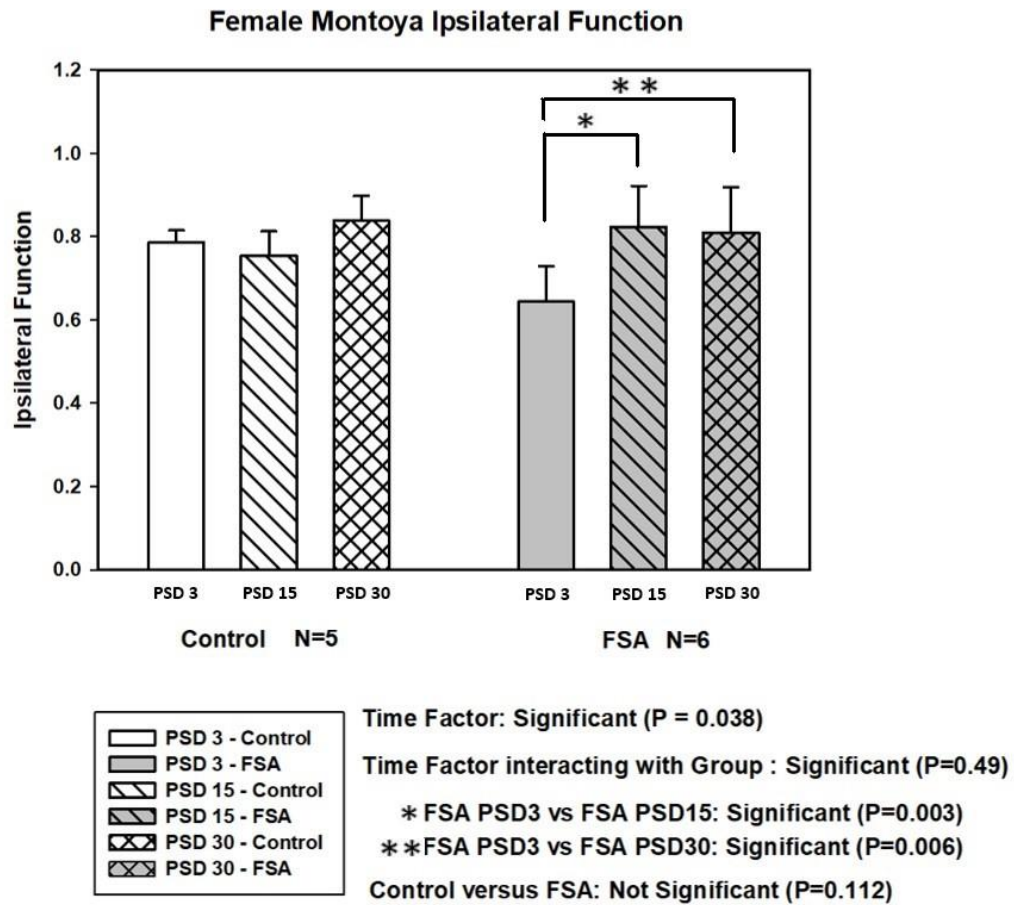
<b>Group</b>	<b>Number of Rats Included in Ipsilateral Analysis</b>	<b>Number of Rats included in Contralateral Analysis</b>
Male Control	7	8
Male FSA	7	9
Female Control	5	8
Female FSA	6	7

Figure 8 illustrates the male ipsilateral function for the control and FSA groups at PSD 3, 15, and 30. There were no statistically significant differences identified between the control and FSA groups ( $P = 0.139$ ). For the control animals, a statistically significant increase was observed from PSD 3 ( $0.739 \pm 0.0417$ ) to PSD 30 ( $1.036 \pm 0.0573$ ) ( $P < 0.001$ ). There was a trend for an increase from PSD 3 ( $0.739 \pm 0.0417$ ) to PSD 15 ( $0.857 \pm 0.0783$ ) in the control group, but this difference was not statistically significant ( $P = 0.041$ , Critical  $P = 0.025$ ). In the FSA group, a trend for an increase in function was observed from PSD 3 ( $0.731 \pm 0.0533$ ) to PSD 15 ( $0.826 \pm 0.0534$ ) and PSD 3 ( $0.731 \pm 0.0533$ ) to PSD 30 ( $0.823 \pm 0.0353$ ), but these were not statistically significant.



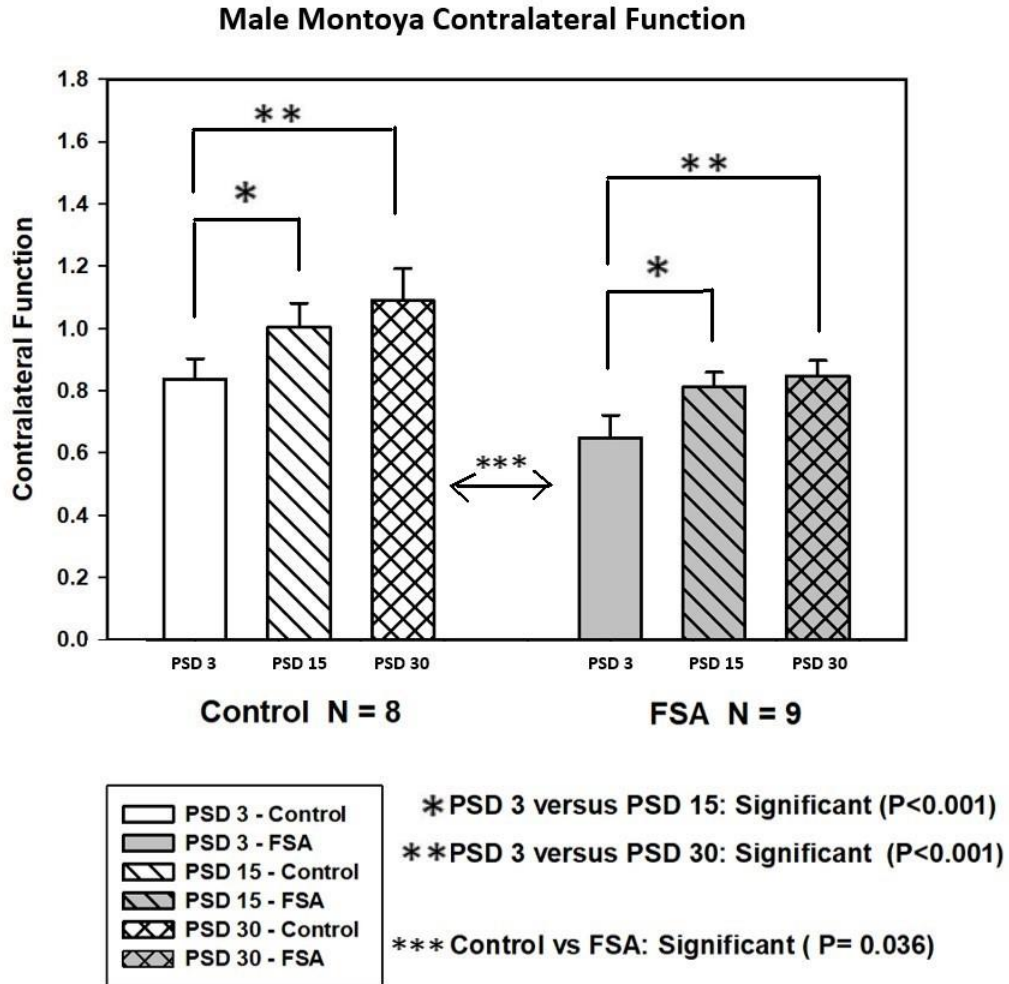
**Figure 8:** Male Montoya Staircase ipsilateral function results comparing control group ( $N = 7$ ) to Fluoxetine/Simvastatin/Ascorbic acid (FSA) drug combination group ( $N = 7$ ). The x-axis denotes the two groups at three time periods (PSD 3, PSD 15, and PSD 30). The y-axis denotes the ipsilateral paw function; 1.0 = normalized pre-surgery ipsilateral function. A repeated measures two-way ANOVA was performed to determine if differences were statistically significant. Error bars represent SEM. Graph was created using SigmaPlot software.

In Figure 9, the female ipsilateral function for the control and FSA groups at PSD 3, 15, and 30 can be seen. No statistically significant differences were identified between the control and FSA groups ( $P = 0.112$ ). For FSA animals, a statistically significant increase was observed from PSD 3 ( $0.643 \pm 0.0860$ ) to PSD 15 ( $0.823 \pm 0.0985$ ) ( $P = 0.003$ ) and PSD 3 ( $0.643 \pm 0.0860$ ) to PSD 30 ( $0.810 \pm 0.109$ ) ( $P = 0.006$ ). A trend for an increase from PSD 3 ( $0.786 \pm 0.0293$ ) to PSD 30 ( $0.838 \pm 0.0593$ ) and from PSD 15 ( $0.754 \pm 0.0591$ ) to PSD 30 ( $0.838 \pm 0.0593$ ) was observed in the control group, but the differences were not statistically significant ( $P = 0.386$  and  $P = 0.169$ , respectively).



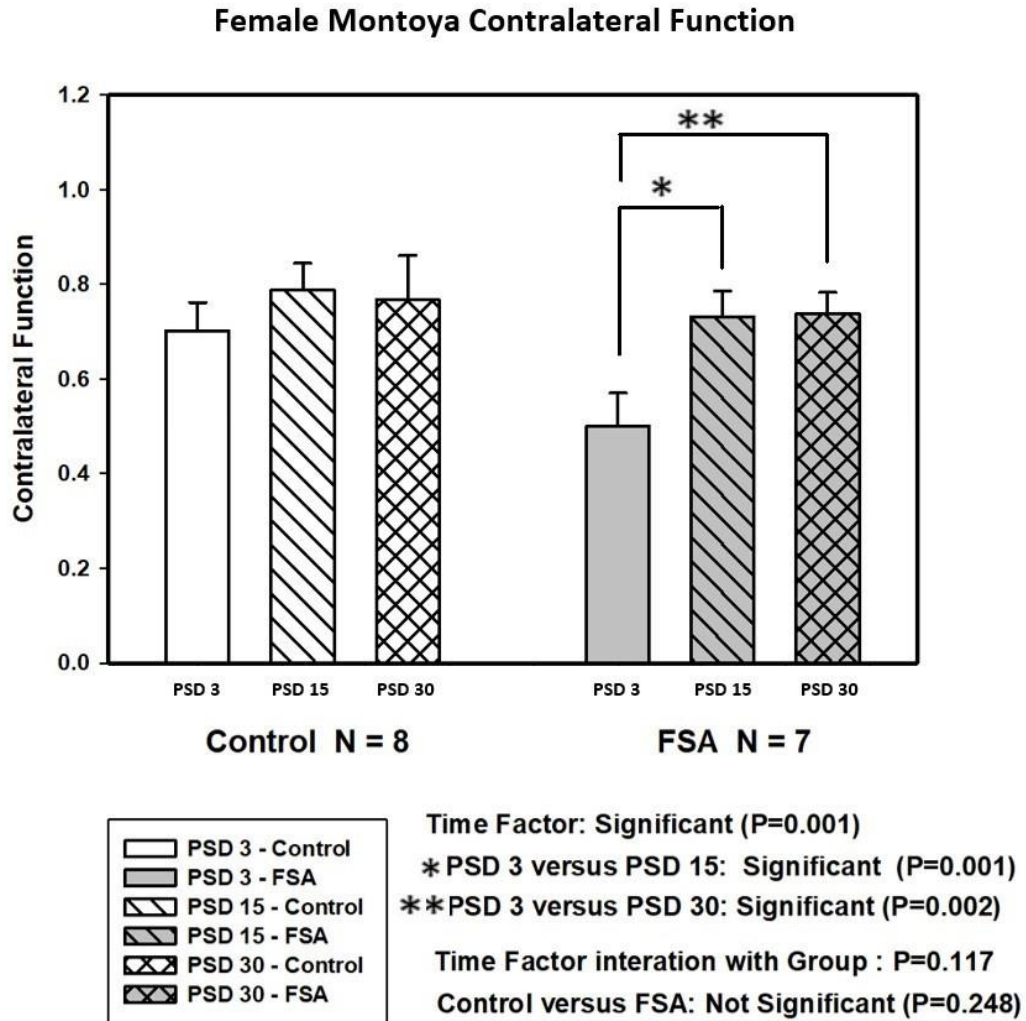
**Figure 9:** Female Montoya Staircase ipsilateral function results comparing control group (N = 5) to Fluoxetine/Simvastatin/Ascorbic acid (FSA) drug combination group (N = 6). The x-axis denotes the two groups at three time periods (PSD 3, PSD 15, and PSD 30). The y-axis denotes the ipsilateral paw function; 1.0 = normalized pre-surgery ipsilateral function. A repeated measures two-way ANOVA was performed to determine if differences were statistically significant. Error bars represent SEM. Graph was created using SigmaPlot software.

Figure 10 shows the male contralateral function for the control and FSA groups at PSD 3, 15, and 30. A statistically significant difference was observed between the control and FSA groups ( $P = 0.036$ ), with control animals showing greater contralateral function. For control animals, statistically significant increases in function were seen PSD 3 ( $0.838 \pm 0.0652$ ) to PSD 15 ( $1.003 \pm 0.0785$ ) and PSD 3 ( $0.838 \pm 0.0652$ ) to PSD 30 ( $1.089 \pm 0.103$ ) ( $P < 0.001$ ). The FSA group also exhibited statistically significant increases in contralateral function from PSD 3 ( $0.649 \pm 0.0726$ ) to PSD 15 ( $0.811 \pm 0.0472$ ) and PSD 3 ( $0.649 \pm 0.0726$ ) to PSD 30 ( $0.848 \pm 0.0489$ ) ( $P < 0.001$ ).



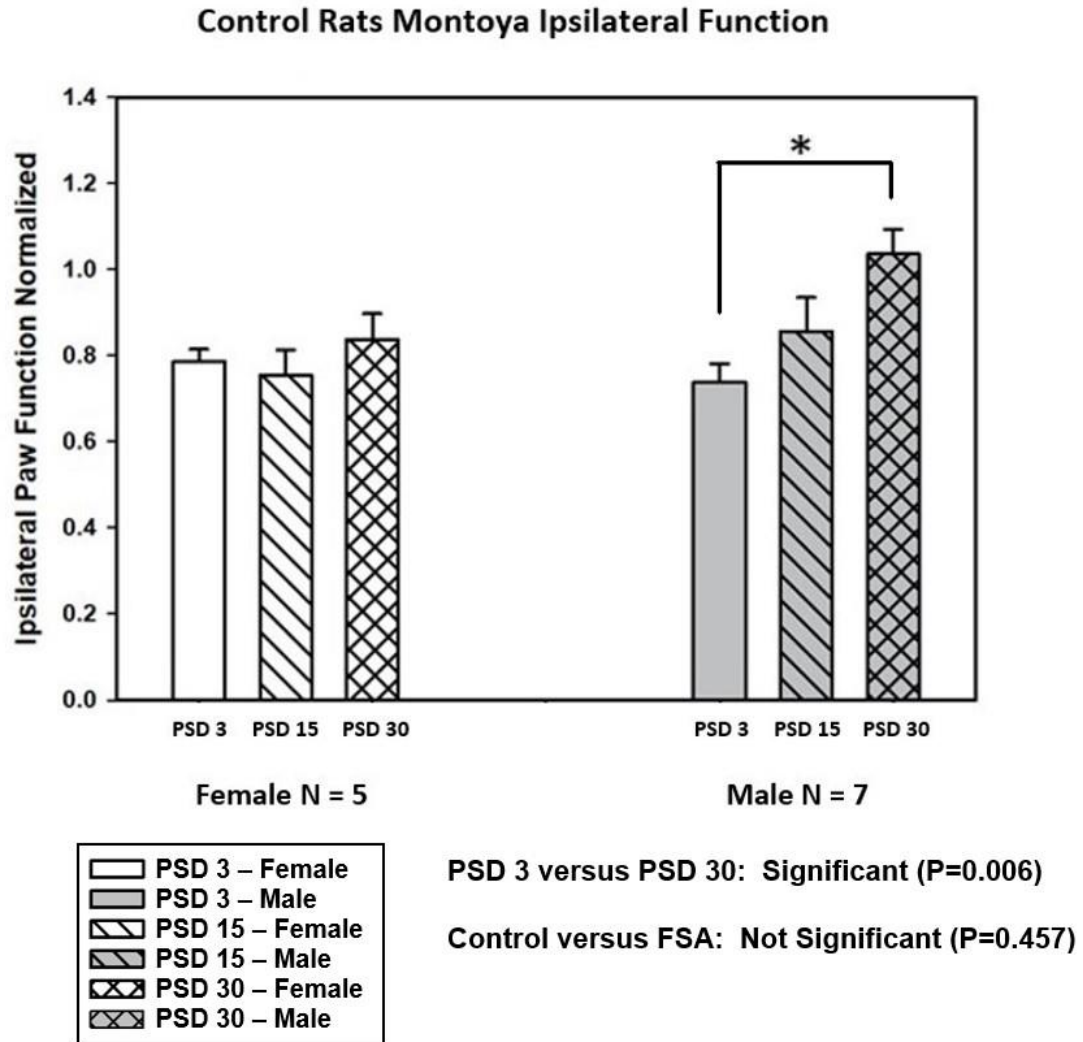
**Figure 10:** Male Montoya Staircase contralateral function results comparing control group (N = 8) to Fluoxetine/Simvastatin/Ascorbic acid (FSA) drug combination group (N = 9). The x-axis denotes the two groups at three time periods (PSD 3, PSD 15, and PSD 30). The y-axis denotes the contralateral paw function; 1.0 = normalized pre-surgery contralateral function. A repeated measures two-way ANOVA was performed to determine if differences were statistically significant. Error bars represent SEM. Graph was created using SigmaPlot software.

Figure 11 depicts the female contralateral function for the control and FSA groups at PSD 3, 15, and 30. No statistically significant differences were found between the control and FSA groups ( $P = 0.248$ ). For FSA animals, a statistically significant increase in function was observed PSD 3 ( $0.500 \pm 0.0703$ ) to PSD 15 ( $0.731 \pm 0.0550$ ) ( $P = 0.001$ ) and PSD 3 ( $0.500 \pm 0.0703$ ) to PSD 30 ( $0.739 \pm 0.0445$ ) ( $P = 0.002$ ). In the control group, a trend for an increase in function was observed PSD 3 ( $0.703 \pm 0.0590$ ) to PSD 15 ( $0.789 \pm 0.0563$ ) and PSD 3 ( $0.703 \pm 0.0590$ ) to PSD 30 ( $0.767 \pm 0.0935$ ), but these were not statistically significant.



**Figure 11:** Female Montoya Staircase contralateral function results comparing control group (N = 8) to Fluoxetine/Simvastatin/Ascorbic acid (FSA) drug combination group (N = 7). The x-axis denotes the two groups at three time periods (PSD 3, PSD 15, and PSD 30). The y-axis denotes the contralateral paw function; 1.0 = normalized pre-surgery contralateral function. A repeated measures two-way ANOVA was performed to determine if differences were statistically significant. Error bars represent SEM. Graph was created using SigmaPlot software.

Figure 12 depicts the innate differences seen between male and female animals in recovery with aging. There was a trend for an increase in male ipsilateral paw function with time (PSD 3:  $0.739 \pm 0.0417$ , PSD 15:  $0.857 \pm 0.0783$ , PSD 30:  $1.036 \pm 0.0573$ ), whereas female ipsilateral paw function did not show an increasing trend (PSD 3:  $0.786 \pm 0.0293$ , PSD 15:  $0.754 \pm 0.0591$ , PSD 30:  $0.838 \pm 0.0593$ ). This shows that the female middle-aged rats were not naturally recovering (full recovery was not seen), while the males were (full recovery was seen). Statistically significant difference was seen PSD 3 versus PSD 30 for males ( $P = 0.006$ ).



**Figure 12:** Female control versus male control Montoya Staircase ipsilateral paw function following focal demyelination with lysolecithin injection. The x-axis denotes the two groups (female control and male control) at three time periods (PSD 3, PSD 15, and PSD 30). The y-axis denotes the ipsilateral paw function; 1.0 = normalized pre-surgery ipsilateral function. A repeated measures two-way ANOVA was performed to determine if differences were statistically significant. Error bars represent SEM. Graph was generated using SigmaPlot software.

### ***DCX Staining Analysis***

DCX staining was used as a marker for neurogenesis in the subventricular zone. Multiple images of each brain slice were taken using the bright-field optical microscope with 40X magnification (4X objective and 10X ocular) to capture the DCX staining along the subventricular zone of the lateral ventricles. Images were combined in Adobe Photoshop to create a single seamless image of each slice with both ventricles present. Figure 13 illustrates one such image with the dark purple colored DCX staining seen on the outside of the ventricles. Images were converted into grayscale, then analyzed in the NIH Image J software.

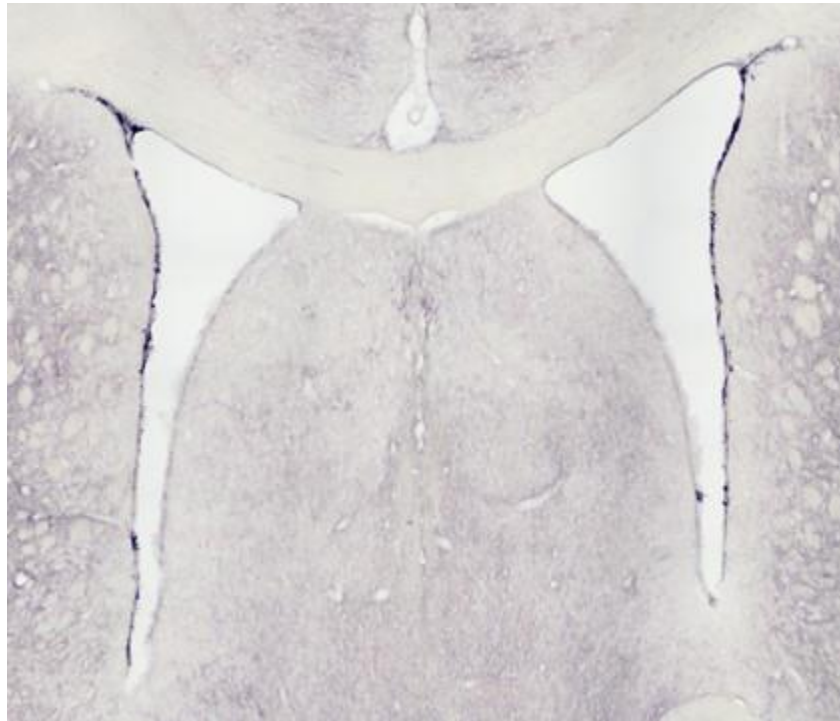


***Figure 13:*** Image of MS27 ventricles with dark purple DCX staining. Images of magnified sections of the ventricles and surrounding area were stitched together using Adobe Photoshop to create this image.

The brain slices from one male animal and one female animal were initially used to test different dilutions of staining. As these two animals did not show functional deficits, they were excluded from all subsequent analysis. Staining did not work on coronal slices for five male animals; therefore, they were also excluded from DCX analysis. One additional female animal was excluded from DCX analysis due to insufficient number of coronal slices available for analysis. Table 4 shows the test groups remaining for final DCX analysis once exclusions were applied.

**Table 4:** *Test groups for final DCX analysis following application of exclusions.*

<b>Group</b>	<b>Number of Rats included in DCX Analysis</b>
Male Control	6
Male FSA	6
Female Control	7
Female FSA	9

Additionally, there was staining seen in the corpus callosum above the right ventricle in a few animals. Figure 14 illustrates this staining (red arrow pointing to stain). The site of DCX stain corresponds to the site of the injury in the corpus callosum. The amount of staining in the corpus callosum was also quantified, however it was not included in the DCX analysis.



**Figure 14:** DCX stain in the corpus callosum above the right ventricle of MS6 (male FSA group), indicated by the red arrow. Images of magnified sections of the ventricles and surrounding area were stitched together and converted into grayscale using Adobe Photoshop to create this image.

The average amount of DCX on each ventricle per 50  $\mu\text{m}$  coronal slice was quantified as an average DCX density (shown in Figure 15) and a total DCX volume (shown in Figure 16). Male animals (both control and FSA) showed significantly more DCX per ventricle than female animals ( $P < 0.001$ ). The mean DCX density for the male control group was  $5.675 \pm 0.318 \text{ mm}^2/\text{ventricle}$ , male FSA was  $4.544 \pm 0.288 \text{ mm}^2/\text{ventricle}$ , female control was  $3.253 \pm 0.268 \text{ mm}^2/\text{ventricle}$ , and female FSA was  $3.094 \pm 0.216 \text{ mm}^2/\text{ventricle}$ . Significant differences were also seen in control versus FSA groups ( $P = 0.025$ ).

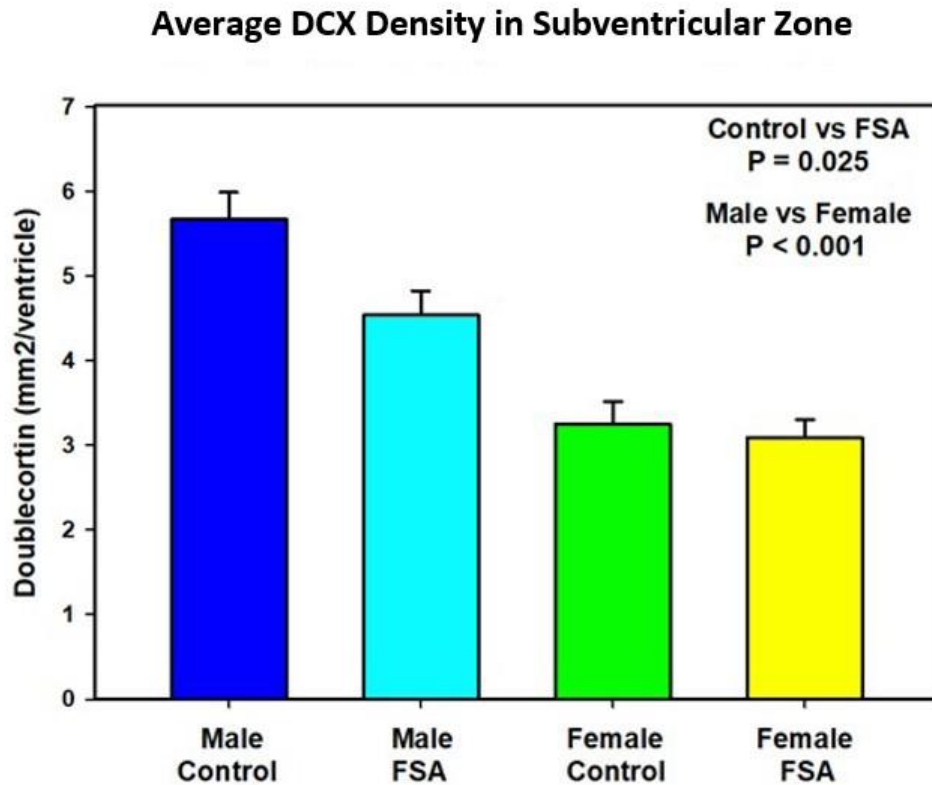


**Figure 15:** Average DCX density in the subventricular zone for male and female groups. The amount of DCX is measured in mm<sup>2</sup> per ventricle. The blue bar is the male control group (N = 6), the cyan bar is the male FSA group (N = 6), the green bar is the female control group (N = 7), and the yellow bar is the female FSA group (N = 9). Error bars represent SEM. Significant differences found in control versus FSA (P = 0.025) and male versus female (P < 0.001). Graph was generated using SigmaPlot software.

Figure 16 shows the volume of DCX in the subventricular zone (in  $\text{mm}^3$ ). This measurement was obtained by multiplying the area of DCX by 0.05 to account for the 50-micron thickness of the brain slices, then multiplying by 8, as each brain was sliced into 8 different sections (vials) for staining. DCX volume was greater in control groups (male:  $48.816 \pm 2.941 \text{ mm}^3$ , female:  $30.437 \pm 1.872 \text{ mm}^3$ ) than FSA groups (male:  $40.310 \pm 6.665 \text{ mm}^3$ , female:  $28.817 \pm 1.632 \text{ mm}^3$ ), but the difference was not significant ( $P = 0.154$ ). There was a significant difference in male versus female animals ( $P < 0.001$ ), with males expressing greater DCX volume.

### DCX Volume in Subventricular Zone

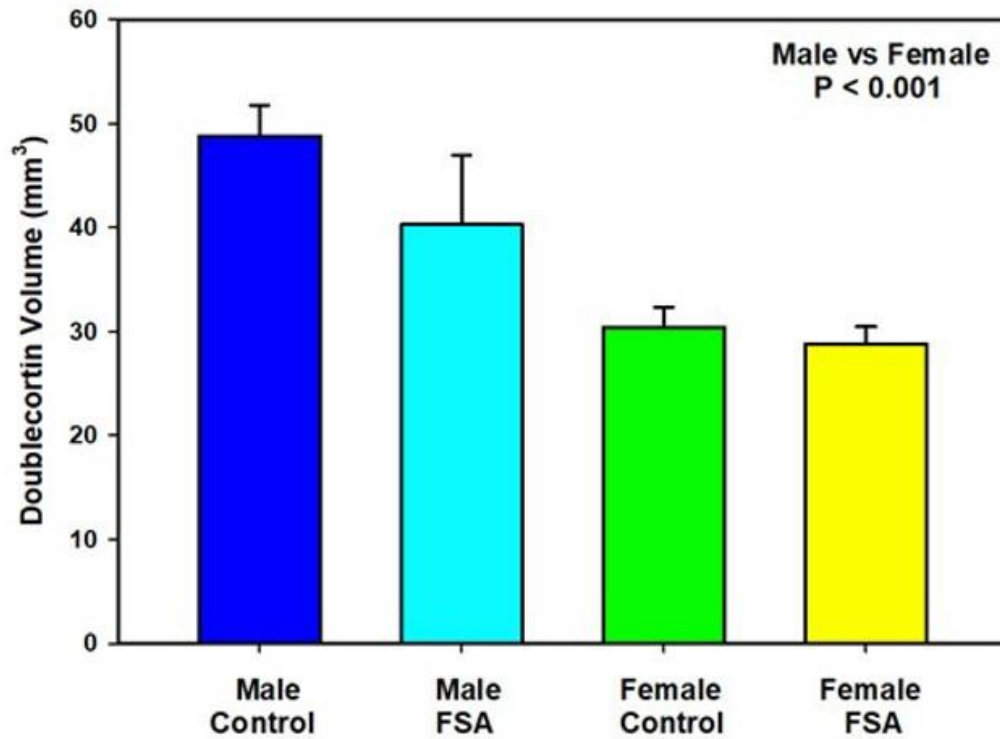


*Figure 16: DCX volume in the subventricular zone for male and female groups. DCX volume is measured in mm<sup>3</sup>. The blue bar is the male control group (N = 6), the cyan bar is the male FSA group (N = 6), the green bar is the female control group (N = 7), and the yellow bar is the female FSA group (N = 9). Error bars represent SEM. Significant differences found in male versus female (P < 0.001). Graph was generated using SigmaPlot software.*

### *Correlating DCX Staining and Functional Recovery*

Correlations between doublecortin volume and ipsilateral functional recovery at PSD 30 (equation for calculation described in Methods) for male rats are depicted in Figure 17. The R value for the male control group was -0.6168, and  $R^2 = 0.3804$ . The R value for the male FSA group was 0.7191, and  $R^2 = 0.5171$ . These values indicate a moderate negative correlation between ipsilateral functional recovery and DCX volume in the control group ( $P = 0.2685$ ), and a moderate positive correlation in the FSA group ( $P = 0.1709$ ), but neither reached statistical significance.

**Male Rats**  
**Correlation between DCX Volume and Ipsilateral Recovery**

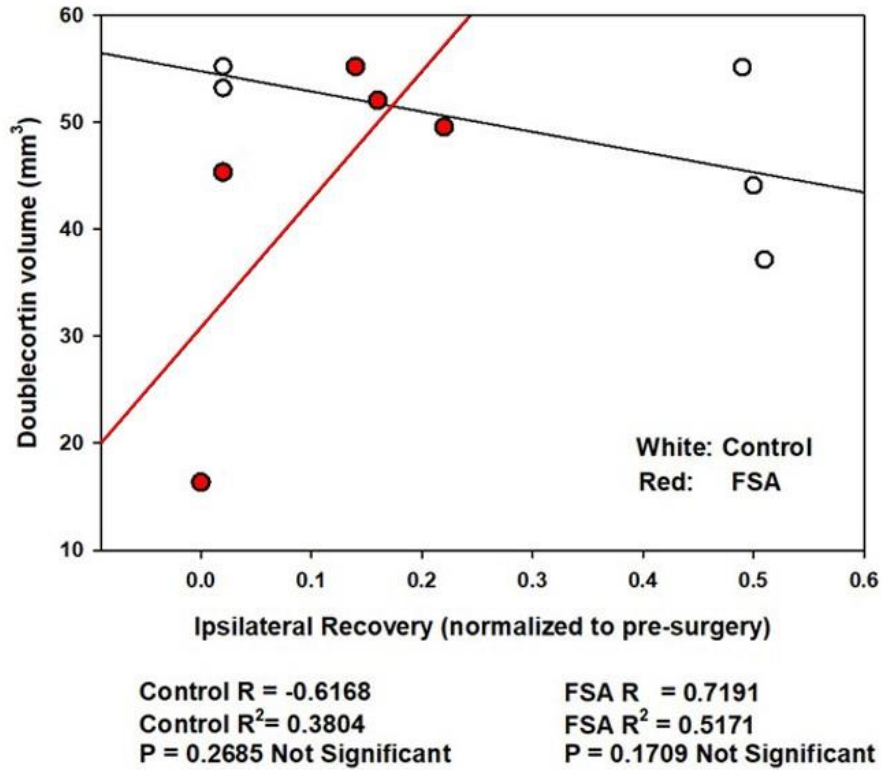


**Figure 17:** Correlations between DCX volume and ipsilateral recovery in male rats.

White circles indicate control animals ( $N = 5$ ), red circles indicate FSA animals ( $N = 5$ ).

The x-axis denotes the ipsilateral functional recovery at PSD 30. The y-axis denotes doublecortin volume in  $\text{mm}^3$ . Graph was generated using SigmaPlot software.

Figure 18 depicts correlations between DCX volume and ipsilateral recovery at PSD 30 (equations for recovery in Methods) in female rats. The R value for the female control group was 0.4418, and  $R^2 = 0.1952$ . The R value for the female FSA group was 0.2331, and  $R^2 = 0.0543$ . These values indicate a non-statistically significant moderate positive correlation between ipsilateral functional recovery and DCX volume in the control group ( $P = 0.4563$ ), and a non-statistically significant low positive correlation in the FSA group ( $P = 0.65668$ ).

**Female Rats**  
**Correlation between DCX Volume and Ipsilateral Recovery**  
**(with FSA group outlier)**

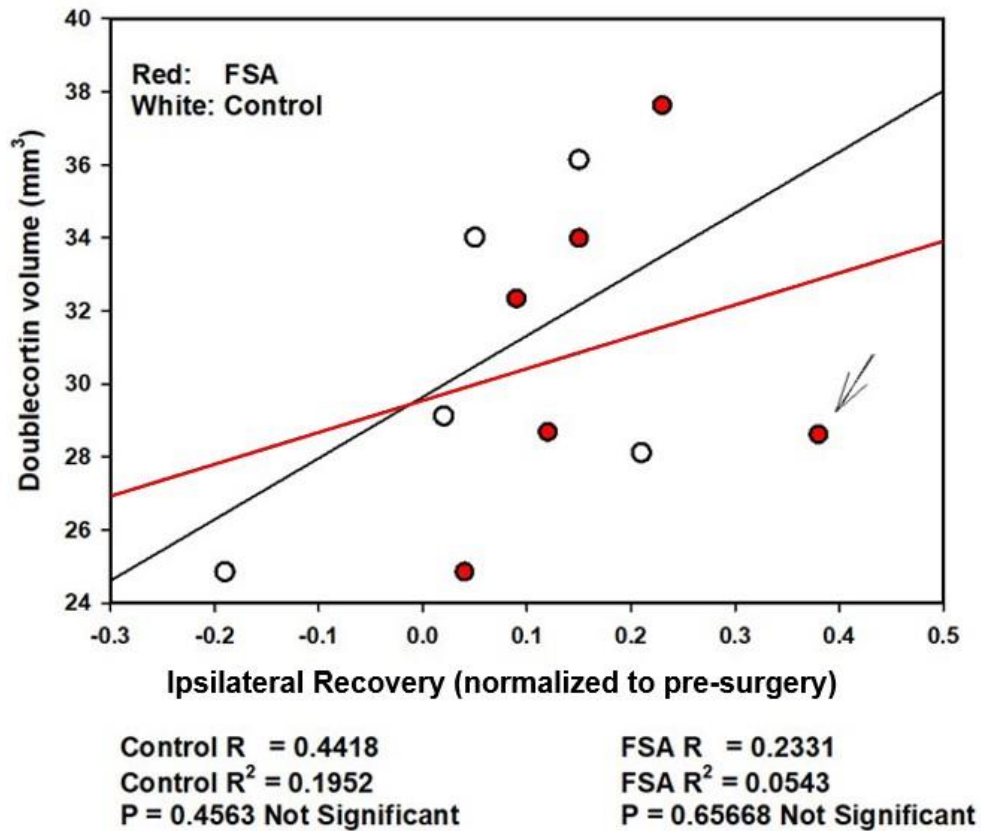


*Figure 18: Correlations between DCX volume and ipsilateral recovery in female rats. White circles indicate control animals (N = 5), red circles indicate FSA animals (N = 6). The x-axis denotes the ipsilateral functional recovery at PSD 30. The y-axis denotes DCX volume in mm<sup>3</sup>. Graph was generated using SigmaPlot software.*

One outlier was identified in the female FSA group from Figure 18. A graph was created after removing the outlier (Figure 19). The R value and  $R^2$  remained the same for the control group ( $R = 0.4418$ ,  $R^2 = 0.1952$ ), but the FSA group showed significant changes. For the FSA group, the R value was 0.9006 and  $R^2 = 0.8111$ . These values show a high significant positive correlation between DCX volume and ipsilateral recovery ( $P = 0.03705$ ).

**Female Rats**  
**Correlation between DCX Volume and Ipsilateral Recovery**

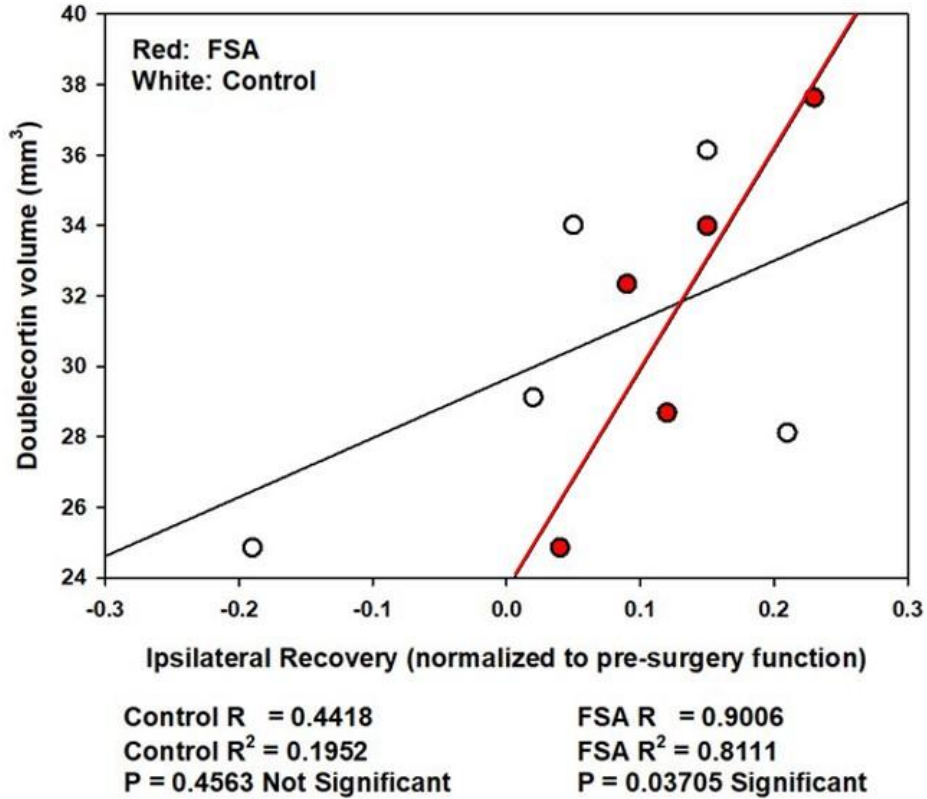


**Figure 19:** Correlations between DCX volume and ipsilateral recovery in female rats with outlier removed. White circles indicate control animals ( $N = 5$ ), red circles indicate FSA animals ( $N = 5$ ). The x-axis denotes the ipsilateral functional recovery at PSD 30. The y-axis denotes DCX volume in  $\text{mm}^3$ . Graph was generated using SigmaPlot software.

Correlational analysis was also conducted for contralateral functional recovery. Figure 20 depicts correlations between contralateral functional recovery at PSD 30 and DCX volume in male rats. The R value for the male control group was -0.9054, and  $R^2 = 0.8197$ . The R value for the male FSA group was 0.6005, and  $R^2 = 0.3606$ . These values indicate a statistically significant high negative correlation between contralateral functional recovery and DCX volume in the control group ( $P = 0.0346$ ), and a moderate positive correlation in the FSA group ( $P = 0.2842$ ), which did not reach statistical significance.

**Male Rats**  
**Correlation between DCX Volume and Contralateral Recovery**

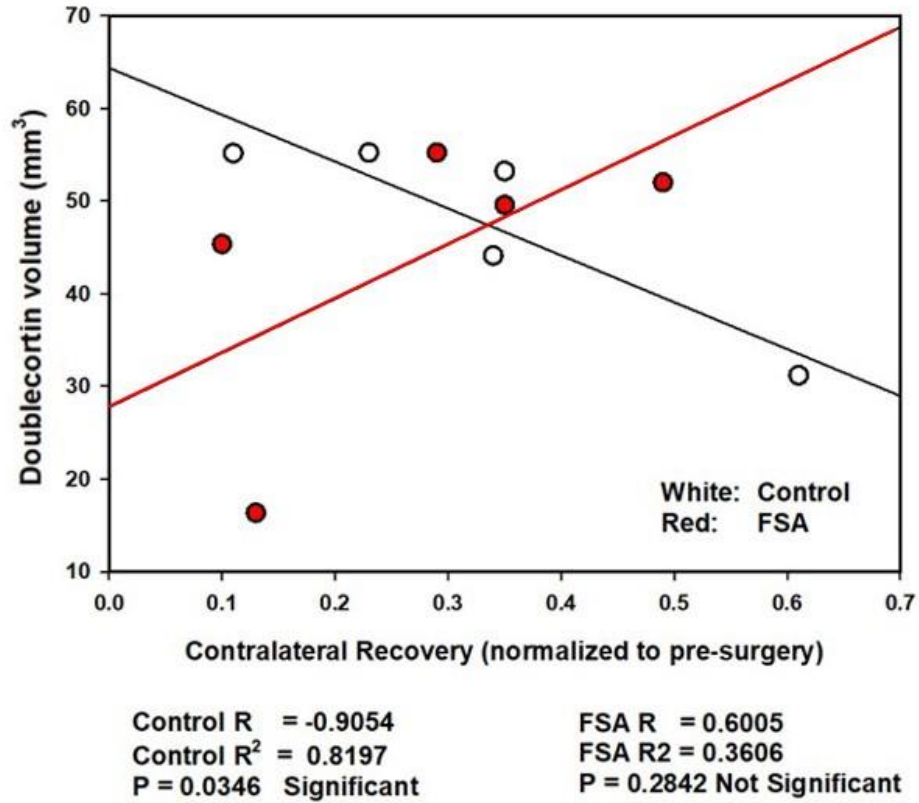


**Figure 20:** Correlations between DCX volume and contralateral recovery in male rats. White circles indicate control animals (N = 5), red circles indicate FSA animals (N = 5). The x-axis denotes the contralateral functional recovery at PSD 30. The y-axis denotes doublecortin volume in mm<sup>3</sup>. Graph was generated using SigmaPlot software.

Figure 21 depicts correlations between contralateral functional recovery at PSD 30 and DCX volume in female rats. The R value for the female control group was -0.0574, and  $R^2 = 0.0033$ . The R value for the female FSA group was 0.3059, and  $R^2 = 0.0936$ . These values indicate no correlation between contralateral functional recovery and DCX volume in the control group ( $P = 0.9145$ ), and a low to moderate positive correlation in the FSA group ( $P = 0.5046$ ), but neither reached statistical significance.

**Female Rats**  
**Correlation between DCX Volume and Contralateral Recovery**

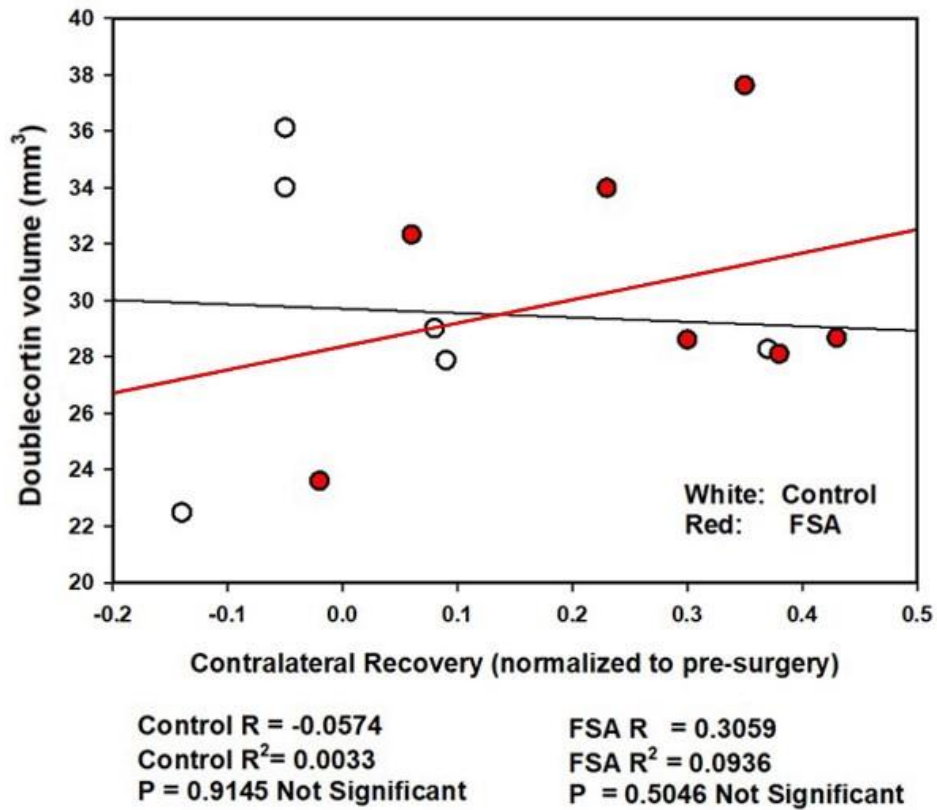


**Figure 21:** Correlations between DCX volume and contralateral recovery in female rats. White circles indicate control animals (N = 6), red circles indicate FSA animals (N = 7). The x-axis denotes the contralateral functional recovery at PSD 30. The y-axis denotes doublecortin volume in mm<sup>3</sup>. Graph was generated using SigmaPlot software.

#### **IV. DISCUSSION**

Multiple sclerosis is an inflammatory disease that leads to demyelination and axonal damage in the central nervous system. Currently, approved therapies primarily target relapsing-remitting MS by modulating immune cells to reduce the immune response (56). While this strategy can help decrease inflammation, it does not appear to provide aid in the progression of the disease. Therapies that promote remyelination of axons should provide an improved strategy for aiding in the recovery of demyelinated white matter tracts, and potentially recovery of lost function. The present experiment examined the drug combination of fluoxetine (5 mg/kg), simvastatin (1 mg/kg), and ascorbic acid (50 mg/kg) on neurogenesis and remyelination in lysolecithin-induced demyelination of the corpus callosum below the right forelimb motor cortex in middle-aged Sprague Dawley rats. This combination was chosen because it has been shown to increase neurogenesis and functional recovery in an ischemic stroke model (32).

Middle-aged male and female rats (10-11 months) were chosen for this experiment as they most accurately represent the human population suffering from progressive forms of MS. It has been seen that disease onset at an older age (40-50 years old) is associated with higher risk of initial primary progressive disease course, and earlier conversion to secondary progressive MS (1). As aging is associated with a decrease in neurogenesis, increasing neurogenesis was presumed to be an essential first step in the repair process, followed by remyelination from newly matured oligodendrocytes. Functional recovery was expected to follow remyelination. Fluoxetine

was used in this experiment in order to transition M1 microglia into M2 microglia, which increases the expression of anti-inflammatory cytokines and growth factors and aids in the reduction of inflammation. Simvastatin was included, as it has been shown to increase the expression of BDNF, which is associated with increased neurogenesis (24, 37). Simvastatin has also been shown to potentially increase proliferation and differentiation of OPCs (24, 38), which is necessary for remyelination to take place. Ascorbic acid was the last drug in the combination, and was included as it has been shown to promote differentiation of OPCs into mature oligodendrocytes, which then have the potential to become myelinating oligodendrocytes (33, 51). If the drugs act as expected and increase neurogenesis and remyelination, full functional recovery would be anticipated in the drug treated animals.

In the male and female rats, both ipsilateral and contralateral function were affected by the demyelinating surgery (shown in Table 2). One potential confounding factor in the interpretation of the results were the differences seen in initial percent deficit at day 3 post surgery (to be discussed further below). White matter tract damage (damage to the corpus callosum) was expected to appear on the same side as the injury (ipsilateral side). Contralateral injury was due to damage in the right cortical region as a result of the injection.

### ***Male Functional Recovery and Neurogenesis***

Ipsilateral function for the male animals increased from PSD 3 to PSD 30 in the control and FSA groups, indicating a recovery over that time, although the differences seen between the control and FSA groups were not statistically significant (Figure 8). The

control group showed a clear increase in function from PSD 3 to PSD 15 to PSD 30, which was expected, as male animals still produce testosterone at this age, and thus neurogenesis should have been continuing to occur naturally (57). The control animals had returned to baseline function by PSD 30. For the FSA group, there was a trend for an increase in function from PSD 3 to PSD 15 and PSD 3 to PSD 30, but full recovery was not reached. Consistent with the observed functional recovery, male control animals had significantly higher measured DCX density (Figure 15) and a trend for greater DCX volume (Figure 16) in the SVZ, relative to the male FSA group. Thus, in the present study, the drug combination in male rats appeared to negatively impact neurogenesis and/or the remyelination process and subsequent functional recovery.

In a previous study using a stroke model in male middle-aged rats, DCX staining was increased relative to control animals using this drug combination (32), however functional recovery was not assessed. In contrast, in a separate study using non-injured male middle-aged rats, fluoxetine or simvastatin independently decreased stem/progenitor cell proliferation (measured by Ki67 staining) in the SVZ, while the combination of fluoxetine, simvastatin, and ascorbic acid did not show any differences from control animals (33). Similar findings have been reported in male rats (8-month-old) and mice (8-week-old) following administration of fluoxetine (58, 59). While the exact reason for the differences among these studies is unclear, the specific models used, uninjured or injured and type of injury, and the power to detect relatively small treatment related effect sizes may be contributing factors. Although controversial, one potential mechanism through which fluoxetine may be exerting an effect in the FSA group relates to its ability to lower testosterone levels, as seen both in human and rodent studies (60-

62). If fluoxetine were to lower testosterone during the recovery phase, one would anticipate a blunted response relative to the control animals.

Contralateral function for the male animals increased significantly over the course of the experiment (Figure 10). The male control group showed full functional recovery by PSD 15 and PSD 30, which, like the ipsilateral male control group, was expected due to the continued production of testosterone. The FSA group also exhibited statistically significant increases in contralateral function from PSD 3 to PSD 15 and PSD 3 to PSD 30, however full recovery was not seen. The contralateral deficit seen in the male FSA group appeared larger than the deficit seen in the control group, indicating a potential increase in deficit caused by the drug combination.

In order to better understand the relationship between DCX staining and functional recovery, correlational analyses were performed. Whereas the male control animals showed the highest values of DCX density or volume, and was the only group to recover full function, there was no significant correlation between DCX volume and ipsilateral functional recovery (Figure 17). Evaluation of the relationship between DCX volume and contralateral functional recovery shows a moderate correlation for the male FSA group, however this was not significant. For the male control group, a significant negative correlation was seen (Figure 20). A potential explanation for the significant negative correlation would be the migration of DCX expressing cells away from the SVZ. Because DCX was only measured in the SVZ, cells that had already migrated to other areas, such as the cortex following injury from the injection, would not be represented in the analysis of DCX. As DCX is expressed in newly formed and migrating neuroblasts, but only transiently so, and then decreases as the neuroblast matures, an increased DCX

expression would be expected to be a precursor to, and thus precede, functional recovery. Thus, another possible explanation for the lack of significant correlation in male animals, control or FSA, would be the timing of the assessment. For example, in the male control animals, ipsilateral functional recovery had returned fully to baseline by day 30, which would indicate the remyelination process, or some other compensatory repair process, had been completed by that time, and thus DCX expression, an early marker for neurogenesis, would not be expected to be as high as it would need to be earlier in the repair/neurogenesis process. In order to better understand the relationship between DCX volume and functional recovery, future investigations could sacrifice animals at both intermediate and final time points to explore the timing related dependencies of early neurogenesis and recovery of function.

### ***Female Functional Recovery and Neurogenesis***

Ipsilateral function for the female animals in the drug treatment group increased significantly over time although full functional recovery was not achieved (Figure 9). Male control rats were expected to show an increase in recovery from PSD 3 to PSD 15 and PSD 30 because they are still naturally producing testosterone, which increases neurogenesis and promotes healing (57). The results from Figure 12 support the idea that loss of estrogen at menopause reduces neurogenesis in females. In this figure, it was seen that male control animals recovered over time, while female control animals did not. Sex hormones, especially estrogens and testosterone, have been shown to have neuroprotective effects and stimulate neurogenesis (57, 63-65). As opposed to what was seen in the male rats, the drug combination may have helped increase functional recovery

in the females. Previous work in this lab has also indicated increased function on the Montoya Staircase following FSA drug treatment in stroke-induced female middle-aged rats (32). Alternatively, the ability to detect a significant recovery in the FSA treated females may have resulted from the larger initial deficit seen in this group relative to the control group. Ipsilateral deficits were expected to be seen following the lysolecithin injection below the forelimb motor cortex on the right side of the brain. The deficit seen in the female animals, especially the controls, was not as large as anticipated. Following demyelinating surgery, the function in the female control animals was still around 80%, while the FSA animals had about 65% function. There are several possible explanations for why the discrepancies between control and FSA treated female animals were observed, including: greater initial deficit resulting from lysolecithin injection in FSA versus controls, and/or unexpected side effects of the drug treatment which interfere with early post-surgery repair mechanisms.

Consistent with the ipsilateral functional recovery seen at day 30 in the female groups, DCX density (Figure 15) and DCX volume (Figure 16) in the subventricular zone, at this timepoint, were not different. Furthermore, both female control and female FSA groups showed DCX density and volume well below that observed in the male groups, further supporting the hypothesis that sex hormones are playing a significant role in neurogenesis and functional recovery, as observed previously (32, 33).

In order to better understand the potential contribution of early drug treatment versus initial unequal variance among groups, future investigations could assess day 3 deficit prior to group assignment and initiation of drug treatment. As for potential unanticipated drug effects, fluoxetine enantiomers have previously been shown to have

differential effects on blood brain barrier permeability in male and female, young and old, rats (66). These prior observations raise the possibility that a fluoxetine-mediated increase in blood brain barrier leakage contributed to an early increase in inflammatory infiltrates, resulting in the greater deficit observed in FSA animals at day 3 post-surgery within the present study. Future studies examining different proportions of R-fluoxetine and S-fluoxetine enantiomers, which appear to have differential effects (66) may help determine the cause of these unexpected findings.

Contralateral function for the female animals increased significantly over the course of the experiment, but differences seen between control and FSA groups were not statistically significant (Figure 11). The female control group showed some recovery, but did not return to normal function, which is believed to be due to age related hormonal changes (33). Female Sprague Dawley rats begin their transition into menopause at approximately 8-10 months (67), therefore these rats should have been going through, or gone through, the rat equivalent of menopause and presumably have low estrogen levels. Menopause has been associated with reports of increased disability in MS (7, 68), which could contribute to the lack of full functional recovery seen in the present experiment. In order to assess the impact of hormonal status, a future investigation could include a group of younger female rats and/or treatment group with hormone replacement therapy.

The contralateral deficit seen in the female FSA group appeared larger than the deficit seen in the control group, indicating a potential increase in contralateral deficit caused by the drug combination. As discussed above, fluoxetine (and/or specific R/S enantiomers thereof) may increase blood brain barrier permeability resulting in these unexpected findings (66). Alternatively, the observations seen at day 3 may merely

reflect unequal random variation between groups as a result of the surgery. As previously suggested, group assignment and initiation of drug treatment after day 3 functional deficit testing would be one way to tease apart the potential influence of drug administration on the initially observed deficit, while further exploration of differing ratios of fluoxetine R/S enantiomers may help explain the potential unanticipated drug effects.

The relationship between DCX volume and ipsilateral functional recovery in the female animals trended as initially hypothesized, although statistically significant correlations were not observed, unless, as in the case of the female FSA group, an apparent outlier is removed from the analysis (Figure 19). In contrast, there was no clear relationship between DCX volume and contralateral functional recovery in the female animals (Figure 21). Ultimately, as discussed above for the male animals, any potential relationship between DCX volume and functional recovery may be highly dependent on the timing of assessment. Furthermore, while DCX is generally considered a marker for newly born migrating neurons, there is evidence that OPCs can also express DCX (29). This indicates that some of the DCX staining could be marking migrating OPCs that are headed to the injury site where they would mature and potentially help remyelinate the injured area of the brain. Figure 14 shows an example of the DCX staining in the corpus callosum, which could be oligodendrocytes migrating to the injured area.

Staining with Oligo1 antibody (performed as a preliminary part of the experiment) showed that there are oligodendrocytes in the corpus callosum (see Appendix D). Because full functional recovery is not exhibited in the FSA groups, the oligodendrocytes that have migrated to the corpus callosum might not be wrapping properly around the axons.

Taken together, Oligo1 staining and DCX staining in the corpus collosum indicate that DCX can stain migrating oligodendrocytes, which are moving to the injured area of the brain. Knowing that oligodendrocytes are in fact migrating to the injured area, but functional recovery is not fully demonstrated, suggests that although neurogenesis is occurring, there is potentially something prohibiting remyelination of the damaged axons in the FSA groups. Future studies confirming the presence of OPCs and their potential proliferation in combination with DCX staining and functional recovery may help further explain the disparities observed in the present study.

### *Considerations for Future Studies*

While the results of the present investigation both support and extend previous findings of the potential impact of a drug combination to alter post-injury neurogenesis and functional recovery in a rodent model of MS, additional questions were raised presenting opportunities for future study.

### *Drug Combination and Dosage*

As discussed above, based on previous work, fluoxetine and/or its R/S enantiomers may impact testosterone levels and also influence blood brain barrier permeability and thus impact inflammatory mediator infiltration of the brain (66). Future studies may choose to investigate varying ratios of fluoxetine R/S enantiomers and/or use a different SSRI.

Similarly, there is some controversy over the effectiveness of simvastatin in treating multiple sclerosis. Some studies have shown an increase in oligodendrocyte differentiation following treatment with statins (24, 38), while others have shown statins

to have a detrimental effect on oligodendrocyte survival and remyelination (45). However, the studies showing the detrimental effects tested the drug on male animals, not females. Female rats were shown to have increased stem/progenitor cell proliferation following treatment with simvastatin (33). Furthermore, combining simvastatin with fluoxetine and ascorbic acid was shown to increase neurogenesis in male and female rats in a stroke model, as well as increasing functional recovery in female rats (32). The results from the present experiment indicate simvastatin may be more detrimental to neurogenesis and/or the subsequent remyelination process. Repeating this study with multiple variations of drug dosage combinations could be beneficial in determining the optimal dosage of each drug in increasing neurogenesis and functional recovery. Future studies could also replace simvastatin with a different anti-inflammatory drug, such as ibuprofen. Ibuprofen has been shown to have neuroprotective effects, reduce neuroinflammation, and increase BDNF levels (69-71).

#### *Timing of Group Assignment and Drug Initiation*

As the reason for differences in early functional deficit (PSD 3) in FSA groups relative to control groups is unclear (drug induced, experimental variability, or some combination thereof), future studies may adjust the timing of group assignment and initiation of drug treatment to follow deficit testing on day 3 (72). This experimental design would enable establishment of groups with a similar starting mean deficit and variance, thereby attributing any subsequent differences in recovery measures solely to drug-induced effects.

### Timing of DCX Assessment

In the present investigation, DCX (an early marker of neurogenesis) was only assessed after PSD 30. Inclusion of additional study arms to allow for assessment of DCX at intermediate time points would enable better understanding of the temporal relationship between neurogenesis and recovery of function.

### Number of Animals and Animal Type

In the present study, multiple observations demonstrate trends, but failed to reach statistical significance. Given the variability seen in these measures, and the comparatively small effect sizes, increasing the N for each group would enable greater power to detect whether these trends are true differences. An initial sample size calculation, given the effects and variability across measures, suggest at least a doubling of group size would be needed. Additionally, the number of animals that were excluded from analysis due to lack of significant initial deficit was greater than anticipated. Therefore, future studies could also consider a third injection site of lysolecithin, ensuring the toxin is adequately demyelinating the corpus callosum.

As highlighted in the discussion above, profound gender differences were observed across both key variables (function and DCX staining) in the present study. These differences were largely attributed to the ages of the animals (middle-aged), related sex hormone status, and/or potential drug effects on those hormones. In order to better understand the contribution of hormonal status to the observed outcomes, future studies could measure testosterone and estrogen levels and include arms of male and female animals at various stages of growth/development. Alternatively, an approach using

specific hormone replacement therapy (estrogen) in females, and/or castration in males may also be highly informative.

### ***Conclusion***

Whereas a drug treatment regime that increases neurogenesis and subsequent remyelination would be potentially beneficial to patients suffering from progressive MS, and other white matter injury diseases such as traumatic brain injury and stroke, the results of the present investigation, as with previous research, underscores the importance of understanding the intricacies and complexities of pharmaceutical interventions as they relate to normal versus disease state repair processes, when complicated by gender and age based hormonal differences.

## V. APPENDICES

### Appendix A

#### *Male Montoya Staircase Raw Data*

*Values highlighted in green indicate animals with a deficit lower than 10% and were excluded from analysis. Animals with contralateral deficit values lower than 10% were only excluded if the animal also showed 10% or lower ipsilateral deficit. Sham rats did not perform Montoya Staircase.*

<b>Rat ID</b>	<b>Group</b>	<b>Ipsilateral Deficit (PSD 3)</b>	<b>Contralateral Deficit (PSD 3)</b>	<b>Ipsilateral Recovery (PSD 15)</b>	<b>Contralateral Recovery (PSD 15)</b>	<b>Ipsilateral Recovery (PSD 30)</b>	<b>Contralateral Recovery (PSD 30)</b>
MS1	Control	43%	27%	0%	5%	43%	20%
MS2	FSA	39%	33%	32%	21%	20%	9%
MS3	FSA	-7%	19%	0%	-11%	-7%	-3%
MS4	Control	33%	29%	41%	14%	49%	11%
MS5	Sham						
MS6	FSA	29%	71%	8%	49%	14%	29%
MS7	Control	13%	23%	-20%	14%	2%	23%
MS8	Control	27%	-9%	5%	35%	51%	61%
MS9	FSA	-4%	2%	-6%	2%	2%	-2%
MS10	Control	22%	0%	17%	6%	12%	6%
MS11	FSA	17%	37%	0%	8%	-10%	14%

MS12	Control	-13%	14%	-11%	12%	6%	12%
MS13	FSA	49%	65%	7%	27%	16%	49%
MS14	Control	13%	46%	-4%	27%	2%	35%
MS15	FSA	30%	45%	28%	40%	22%	35%
MS16	FSA	-6%	21%	109%	-2%	34%	23%
MS17	FSA	13%	16%	-15%	-4%	2%	10%
MS18	Sham						
MS19	Control	32%	0%	45%	20%	50%	34%
MS20	FSA	11%	9%	6%	17%	0%	13%

## Appendix B

### *Female Montoya Staircase Raw Data*

*Values highlighted in green indicate animals with a deficit lower than 10% and were excluded from analysis. Sham rats did not perform Montoya Staircase.*

<b>Rat ID</b>	<b>Group</b>	<b>Ipsilateral Deficit (PSD 3)</b>	<b>Contralateral Deficit (PSD 3)</b>	<b>Ipsilateral Recovery (PSD 15)</b>	<b>Contralateral Recovery (PSD 15)</b>	<b>Ipsilateral Recovery (PSD 30)</b>	<b>Contralateral Recovery (PSD 30)</b>
MS21	FSA	21%	34%	6%	15%	15%	17%
MS22	Control	-11%	26%	-14%	0%	11%	-23%
MS23	Control	-8%	35%	0%	29%	19%	43%
MS24	FSA	39%	67%	11%	17%	23%	35%
MS25	FSA	28%	56%	25%	20%	9%	6%
MS26	Control	21%	27%	-10%	20%	2%	8%
MS27	Control	7%	16%	0%	9%	8%	9%
MS28	FSA	4%	2%	-2%	-8%	0%	-29%
MS29	Sham						
MS30	FSA	35%	51%	44%	45%	38%	30%
MS31	FSA	-32%	-11%	0%	-16%	-11%	7%
MS32	FSA	4%	16%	-9%	0%	5%	-2%
MS33	Control	15%	16%	2%	-3%	15%	-5%
MS34	Control	29%	12%	-14%	-12%	5%	-4%
MS35	FSA	4%	8%	-7%	0%	-2%	-4%
MS36	FSA	16%	62%	10%	34%	12%	43%

MS37	Sham						
MS38	Control	27%	45%	2%	16%	21%	37%
MS39	FSA	75%	64%	15%	31%	4%	38%
MS40	Control	15%	61%	4%	8%	-19%	-14%

## Appendix C

### *DCX Staining Raw Data*

*Animals highlighted in green were excluded from DCX analysis due to insufficient number of coronal slices available for analysis, stain not working on certain coronal slices, or the animals being used to test dilutions of stain. DCX was measured in Sham animals, but not included in final analysis. MS1-MS20 were male animals, MS21-MS40 were female animals.*

<b>Rat ID</b>	<b>Group</b>	<b>Average DCX Density</b>	<b>DCX Volume</b>
MS1			
MS2			
MS3			
MS4	Control	6.00	55.17
MS5	Sham	5.15	57.64
MS6	FSA	5.52	55.23
MS7	Control	6.28	55.24
MS8	Control	6.64	37.18
MS9			
MS10			
MS11			
MS12	Control	5.00	47.99
MS13	FSA	4.64	52.01
MS14	Control	5.54	53.22

MS15	FSA	5.16	49.57
MS16	FSA	3.65	23.37
MS17	FSA	4.20	45.35
MS18	Sham	4.63	29.61
MS19	Control	4.59	44.10
MS20	FSA	4.08	16.33
MS21	FSA	3.69	33.99
MS22			
MS23	Control	4.02	35.41
MS24	FSA	4.28	37.63
MS25	FSA	3.67	32.34
MS26	Control	3.15	29.01
MS27	Control	2.90	27.88
MS28	FSA	2.58	24.81
MS29	Sham	3.73	26.83
MS30	FSA	2.47	28.62
MS31			
MS32	FSA	2.95	23.60
MS33	Control	3.35	36.14
MS34	Control	4.25	34.02
MS35	FSA	2.82	24.84
MS36	FSA	2.99	28.68
MS37	Sham	3.21	28.28

MS38	Control	2.93	28.12
MS39	FSA	2.39	24.84
MS40	Control	2.16	22.48

## Appendix D

### *Oligo1 Staining Example*

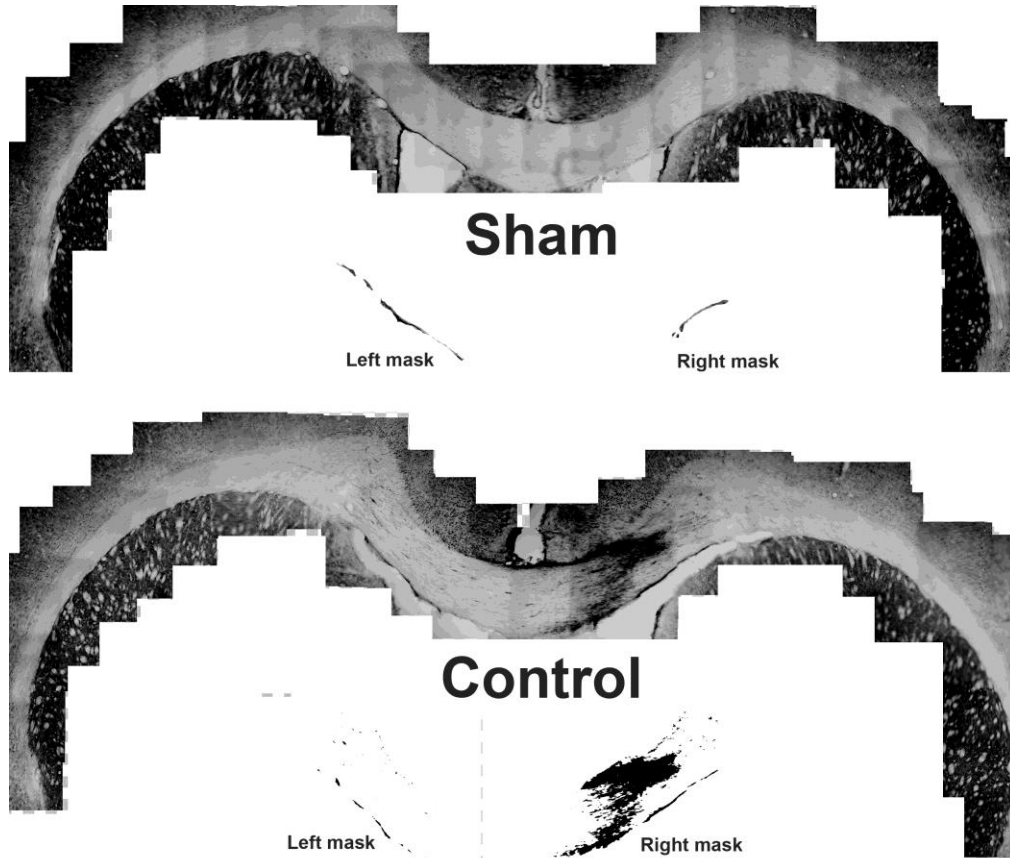


*Image comparing male sham animal stained with Oligo1 image and mask (top) to male control animal stained with Oligo1 image and mask (bottom). Heavy staining in the control animal right side corpus callosum indicates the presence of oligodendrocytes in that area of the brain. This illustrates that oligodendrocytes have migrated to the damaged area of the brain. Scale bar at the bottom set to 150 micrometers.*

## VI. REFERENCES

1. Sanai SA, Saini V, Benedict RH, Zivadinov R, Teter BE, Ramanathan M, et al. Aging and multiple sclerosis. *Mult Scler.* 2016;22(6):717-25.
2. Dobson R, Giovannoni G. Multiple sclerosis - a review. *Eur J Neurol.* 2019;26(1):27-40.
3. Goldenberg MM. Multiple sclerosis review. *P T.* 2012;37(3):175-84.
4. Angeloni B, Bigi R, Bellucci G, Mechelli R, Ballerini C, Romano C, et al. A Case of Double Standard: Sex Differences in Multiple Sclerosis Risk Factors. *Int J Mol Sci.* 2021;22(7).
5. Harbo HF, Gold R, Tintore M. Sex and gender issues in multiple sclerosis. *Ther Adv Neurol Disord.* 2013;6(4):237-48.
6. Ysraelit MC, Correale J. Impact of sex hormones on immune function and multiple sclerosis development. *Immunology.* 2019;156(1):9-22.
7. Voskuhl RR. The effect of sex on multiple sclerosis risk and disease progression. *Mult Scler.* 2020;26(5):554-60.
8. Bove R, Okai A, Houtchens M, Elias-Hamp B, Lugaresi A, Hellwig K, et al. Effects of Menopause in Women With Multiple Sclerosis: An Evidence-Based Review. *Front Neurol.* 2021;12:554375.
9. Lublin FD, Coetzee T, Cohen JA, Marrie RA, Thompson AJ, International Advisory Committee on Clinical Trials in MS. The 2013 clinical course descriptors for multiple sclerosis: A clarification. *Neurology.* 2020;94(24):1088-92.

10. Klineova S, Lublin FD. Clinical Course of Multiple Sclerosis. Cold Spring Harb Perspect Med. 2018;8(9).
11. Lublin FD, Reingold SC, Cohen JA, Cutter GR, Sorensen PS, Thompson AJ, et al. Defining the clinical course of multiple sclerosis: the 2013 revisions. Neurology. 2014;83(3):278-86.
12. National Multiple Sclerosis Society. RRMS. Retrieved from <https://www.nationalmssociety.org/What-is-MS/Types-of-MS>.
13. National Multiple Sclerosis Society. PPMS. Retrieved from <https://www.nationalmssociety.org/What-is-MS/Types-of-MS>.
14. National Multiple Sclerosis Society. SPMS. Retrieved from <https://www.nationalmssociety.org/What-is-MS/Types-of-MS>.
15. Papadopoulos D, Magliozzi R, Mitsikostas DD, Gorgoulis VG, Nicholas RS. Aging, Cellular Senescence, and Progressive Multiple Sclerosis. Front Cell Neurosci. 2020;14:178.
16. Zeydan B, Kantarci OH. Impact of Age on Multiple Sclerosis Disease Activity and Progression. Curr Neurol Neurosci Rep. 2020;20(7):24.
17. Chu F, Shi M, Zheng C, Shen D, Zhu J, Zheng X, et al. The roles of macrophages and microglia in multiple sclerosis and experimental autoimmune encephalomyelitis. J Neuroimmunol. 2018;318:1-7.
18. Saitgareeva AR, Bulygin KV, Gareev IF, Beylerli OA, Akhmadeeva LR. The role of microglia in the development of neurodegeneration. Neurol Sci. 2020;41(12):3609-15.

19. Miranda M, Morici JF, Zanoni MB, Bekinschtein P. Brain-Derived Neurotrophic Factor: A Key Molecule for Memory in the Healthy and the Pathological Brain. *Front Cell Neurosci.* 2019;13:363.
20. Riquelme PA, Drapeau E, Doetsch F. Brain micro-ecologies: neural stem cell niches in the adult mammalian brain. *Philos Trans R Soc Lond B Biol Sci.* 2008;363(1489):123-37.
21. Ming GL, Song H. Adult neurogenesis in the mammalian central nervous system. *Annu Rev Neurosci.* 2005;28:223-50.
22. Curtis MA, Faull RL, Eriksson PS. The effect of neurodegenerative diseases on the subventricular zone. *Nat Rev Neurosci.* 2007;8(9):712-23.
23. Nait-Oumesmar B, Picard-Riera N, Kerninon C, Decker L, Seilhean D, Hoglinger GU, et al. Activation of the subventricular zone in multiple sclerosis: evidence for early glial progenitors. *Proc Natl Acad Sci U S A.* 2007;104(11):4694-9.
24. Xiong Y, Mahmood A, Chopp M. Angiogenesis, neurogenesis and brain recovery of function following injury. *Curr Opin Investig Drugs.* 2010;11(3):298-308.
25. El Waly B, Cayre M, Durbec P. Promoting Myelin Repair through In Vivo Neuroblast Reprogramming. *Stem Cell Reports.* 2018;10(5):1492-504.
26. Mecha M, Feliu A, Carrillo-Salinas FJ, Mestre L, Guaza C. Mobilization of progenitors in the subventricular zone to undergo oligodendrogenesis in the Theiler's virus model of multiple sclerosis: implications for remyelination at lesions sites. *Exp Neurol.* 2013;250:348-52.

27. Picard-Riera N, Decker L, Delarasse C, Goude K, Nait-Oumesmar B, Liblau R, et al. Experimental autoimmune encephalomyelitis mobilizes neural progenitors from the subventricular zone to undergo oligodendrogenesis in adult mice. *Proc Natl Acad Sci U S A*. 2002;99(20):13211-6.
28. Balthazart J, Ball GF. Doublecortin is a highly valuable endogenous marker of adult neurogenesis in canaries. Commentary on Vellema M et al. (2014): Evaluating the predictive value of doublecortin as a marker for adult neurogenesis in canaries (*Serinus canaria*). *J Comparative Neurol* 522:1299-1315. *Brain Behav Evol*. 2014;84(1):1-4.
29. Boulanger JJ, Messier C. Doublecortin in Oligodendrocyte Precursor Cells in the Adult Mouse Brain. *Front Neurosci*. 2017;11:143.
30. Gleeson JG, Lin PT, Flanagan LA, Walsh CA. Doublecortin is a microtubule-associated protein and is expressed widely by migrating neurons. *Neuron*. 1999;23(2):257-71.
31. Brown JP, Couillard-Despres S, Cooper-Kuhn CM, Winkler J, Aigner L, Kuhn HG. Transient expression of doublecortin during adult neurogenesis. *J Comp Neurol*. 2003;467(1):1-10.
32. Corbett AM, Sieber S, Wyatt N, Lizzi J, Flannery T, Sibbit B, et al. Increasing neurogenesis with fluoxetine, simvastatin and ascorbic Acid leads to functional recovery in ischemic stroke. *Recent Pat Drug Deliv Formul*. 2015;9(2):158-66.

33. Sulehria T, Corbett AM, Sharma N, Nagarajan D, Abushamma A, Gagle S, et al. Increasing Progenitor Cell Proliferation in the Sub-Ventricular Zone: A Therapeutic Treatment for Progressive Multiple Sclerosis? *Recent Pat Drug Deliv Formul.* 2020;14(3):233-41.
34. Chung ES, Chung YC, Bok E, Baik HH, Park ES, Park JY, et al. Fluoxetine prevents LPS-induced degeneration of nigral dopaminergic neurons by inhibiting microglia-mediated oxidative stress. *Brain Res.* 2010;1363:143-50.
35. Su F, Yi H, Xu L, Zhang Z. Fluoxetine and S-citalopram inhibit M1 activation and promote M2 activation of microglia in vitro. *Neuroscience.* 2015;294:60-8.
36. Lee JY, Kang SR, Yune TY. Fluoxetine prevents oligodendrocyte cell death by inhibiting microglia activation after spinal cord injury. *J Neurotrauma.* 2015;32(9):633-44.
37. van der Most PJ, Dolga AM, Nijholt IM, Luiten PG, Eisel UL. Statins: mechanisms of neuroprotection. *Prog Neurobiol.* 2009;88(1):64-75.
38. Paintlia AS, Paintlia MK, Khan M, Vollmer T, Singh AK, Singh I. HMG-CoA reductase inhibitor augments survival and differentiation of oligodendrocyte progenitors in animal model of multiple sclerosis. *FASEB J.* 2005;19(11):1407-21.
39. Asahi M, Huang Z, Thomas S, Yoshimura S, Sumii T, Mori T, et al. Protective effects of statins involving both eNOS and tPA in focal cerebral ischemia. *J Cereb Blood Flow Metab.* 2005;25(6):722-9.
40. Liao JK, Laufs U. Pleiotropic effects of statins. *Annu Rev Pharmacol Toxicol.* 2005;45:89-118.

41. Pang PT, Teng HK, Zaitsev E, Woo NT, Sakata K, Zhen S, et al. Cleavage of proBDNF by tPA/plasmin is essential for long-term hippocampal plasticity. *Science*. 2004;306(5695):487-91.
42. Jiang H, Chen S, Li C, Lu N, Yue Y, Yin Y, et al. The serum protein levels of the tPA-BDNF pathway are implicated in depression and antidepressant treatment. *Transl Psychiatry*. 2017;7(4):e1079.
43. Kowianski P, Lietzau G, Czuba E, Waskow M, Steliga A, Morys J. BDNF: A Key Factor with Multipotent Impact on Brain Signaling and Synaptic Plasticity. *Cell Mol Neurobiol*. 2018;38(3):579-93.
44. Hooijmans CR, Hlavica M, Schuler FAF, Good N, Good A, Baumgartner L, et al. Remyelination promoting therapies in multiple sclerosis animal models: a systematic review and meta-analysis. *Sci Rep*. 2019;9(1):822.
45. Miron VE, Zehntner SP, Kuhlmann T, Ludwin SK, Owens T, Kennedy TE, et al. Statin therapy inhibits remyelination in the central nervous system. *Am J Pathol*. 2009;174(5):1880-90.
46. Mori K, Kaneko YS, Nakashima A, Nagasaki H, Nagatsu T, Nagatsu I, et al. Subventricular zone under the neuroinflammatory stress and Parkinson's disease. *Cell Mol Neurobiol*. 2012;32(5):777-85.
47. Czeh B, Muller-Keuker JI, Rygula R, Abumaria N, Hiemke C, Domenici E, et al. Chronic social stress inhibits cell proliferation in the adult medial prefrontal cortex: hemispheric asymmetry and reversal by fluoxetine treatment. *Neuropsychopharmacology*. 2007;32(7):1490-503.

48. Veena J, Rao BS, Srikumar BN. Regulation of adult neurogenesis in the hippocampus by stress, acetylcholine and dopamine. *J Nat Sci Biol Med.* 2011;2(1):26-37.
49. Mirescu C, Gould E. Stress and adult neurogenesis. *Hippocampus.* 2006;16(3):233-8.
50. Corbett A, McGowin A, Sieber S, Flannery T, Sibbitt B. A method for reliable voluntary oral administration of a fixed dosage (mg/kg) of chronic daily medication to rats. *Lab Anim.* 2012;46(4):318-24.
51. Guo YE, Suo N, Cui X, Yuan Q, Xie X. Vitamin C promotes oligodendrocytes generation and remyelination. *Glia.* 2018;66(7):1302-16.
52. McMurran CE, Zhao C, Franklin RJM. Toxin-Based Models to Investigate Demyelination and Remyelination. *Methods Mol Biol.* 2019;1936:377-96.
53. Plemel JR, Michaels NJ, Weishaupt N, Caprariello AV, Keough MB, Rogers JA, et al. Mechanisms of lysophosphatidylcholine-induced demyelination: A primary lipid disrupting myelinopathy. *Glia.* 2018;66(2):327-47.
54. Lafayette Instrument Company. Rat Staircase. Retrieved from <https://lafayetteneuroscience.com/products/rat-staircase>.
55. Vector Laboratories. Using the ABC system. Retrieved from <https://vectorlabs.com/vectastain-elite-abc-kit-standard.html>.
56. Keough MB, Yong VW. Remyelination therapy for multiple sclerosis. *Neurotherapeutics.* 2013;10(1):44-54.
57. Fanaei H, Karimian SM, Sadeghipour HR, Hassanzade G, Kasaeian A, Attari F, et al. Testosterone enhances functional recovery after stroke through promotion of antioxidant defenses, BDNF levels and neurogenesis in male rats. *Brain Res.* 2014;1558:74-83.

58. Guirado R, Sanchez-Matarredona D, Varea E, Crespo C, Blasco-Ibanez JM, Nacher J. Chronic fluoxetine treatment in middle-aged rats induces changes in the expression of plasticity-related molecules and in neurogenesis. *BMC Neurosci.* 2012;13:5.
59. Ohira K, Miyakawa T. Chronic treatment with fluoxetine for more than 6 weeks decreases neurogenesis in the subventricular zone of adult mice. *Mol Brain.* 2011;4:10.
60. Monteiro Filho WO, de Torres SM, Amorim MJ, Andrade AJ, de Moraes RN, Tenorio BM, et al. Fluoxetine induces changes in the testicle and testosterone in adult male rats exposed via placenta and lactation. *Syst Biol Reprod Med.* 2014;60(5):274-81.
61. Bell S, Shipman M, Bystritsky A, Haifley T. Fluoxetine treatment and testosterone levels. *Ann Clin Psychiatry.* 2006;18(1):19-22.
62. Pavlidi P, Kokras N, Dalla C. Antidepressants' effects on testosterone and estrogens: What do we know? *Eur J Pharmacol.* 2021;899:173998.
63. Ponti G, Farinetti A, Marraudino M, Panzica G, Gotti S. Sex Steroids and Adult Neurogenesis in the Ventricular-Subventricular Zone. *Front Endocrinol (Lausanne).* 2018;9:156.
64. Li J, Siegel M, Yuan M, Zeng Z, Finnucan L, Persky R, et al. Estrogen enhances neurogenesis and behavioral recovery after stroke. *J Cereb Blood Flow Metab.* 2011;31(2):413-25.

65. Suzuki S, Gerhold LM, Bottner M, Rau SW, Dela Cruz C, Yang E, et al. Estradiol enhances neurogenesis following ischemic stroke through estrogen receptors alpha and beta. *J Comp Neurol*. 2007;500(6):1064-75.
66. Arkan E. The Effect of Aging on the Blood Brain Barrier Permeability and Response to Fluoxetine Enantiomers [Master of Science Thesis]: Wright State University; 2017.
67. Cruz G, Fernandois D, Paredes AH. Ovarian function and reproductive senescence in the rat: role of ovarian sympathetic innervation. *Reproduction*. 2017;153(2):R59-R68.
68. Bove R, Healy BC, Secor E, Vaughan T, Katic B, Chitnis T, et al. Patients report worse MS symptoms after menopause: findings from an online cohort. *Mult Scler Relat Disord*. 2015;4(1):18-24.
69. Llorens-Martin M, Jurado-Arjona J, Fuster-Matanzo A, Hernandez F, Rabano A, Avila J. Peripherally triggered and GSK-3beta-driven brain inflammation differentially skew adult hippocampal neurogenesis, behavioral pattern separation and microglial activation in response to ibuprofen. *Transl Psychiatry*. 2014;4:e463.
70. Hui CW, Song X, Ma F, Shen X, Herrup K. Ibuprofen prevents progression of ataxia telangiectasia symptoms in ATM-deficient mice. *J Neuroinflammation*. 2018;15(1):308.
71. Lee B, Sur B, Yeom M, Shim I, Lee H, Hahm DH. Effects of systemic administration of ibuprofen on stress response in a rat model of post-traumatic stress disorder. *Korean J Physiol Pharmacol*. 2016;20(4):357-66.

72. Holikova K, Laakso H, Salo R, Shatillo A, Nurmi A, Bares M, et al. RAFF-4, Magnetization Transfer and Diffusion Tensor MRI of Lysophosphatidylcholine Induced Demyelination and Remyelination in Rats. *Front Neurosci.* 2021;15:625167.